

Reference Energies for Double Excitations

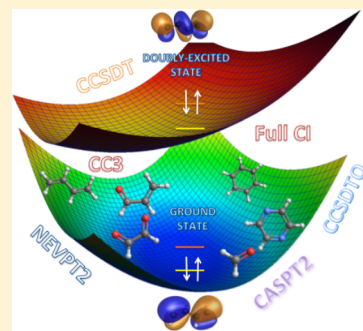
Pierre-François Loos,^{*,†} Martial Boggio-Pasqua,[†] Anthony Scemama,[†] Michel Caffarel,[†]
and Denis Jacquemin[‡]

[†]Laboratoire de Chimie et Physique Quantiques (UMR 5626), Université de Toulouse, CNRS, UPS, 31062 Toulouse, France

[‡]Laboratoire CEISAM (UMR 6230), CNRS, Université de Nantes, 44399 Cedex 3 Nantes, France

Supporting Information

ABSTRACT: Excited states exhibiting double-excitation character are notoriously difficult to model using conventional single-reference methods, such as adiabatic time-dependent density functional theory (TD-DFT) or equation-of-motion coupled cluster (EOM-CC). In addition, these states are typical experimentally “dark”, making their detection in photoabsorption spectra very challenging. Nonetheless, they play a key role in the faithful description of many physical, chemical, and biological processes. In the present work, we provide accurate reference excitation energies for transitions involving a substantial amount of double excitation using a series of increasingly large diffuse-containing atomic basis sets. Our set gathers 20 vertical transitions from 14 small- and medium-size molecules (acrolein, benzene, beryllium atom, butadiene, carbon dimer and trimer, ethylene, formaldehyde, glyoxal, hexatriene, nitrosomethane, nitroxyl, pyrazine, and tetrazine). Depending on the size of the molecule, selected configuration interaction (sCI) and/or multiconfigurational (CASSCF, CASPT2, (X)MS-CASPT2, and NEVPT2) calculations are performed in order to obtain reliable estimates of the vertical transition energies. In addition, coupled cluster approaches including at least contributions from iterative triples (such as CC3, CCSDT, CCSDTQ, and CCSDTQP) are assessed. Our results clearly evidence that the error in CC methods is intimately related to the amount of double-excitation character of the transition. For “pure” double excitations (i.e., for transitions which do not mix with single excitations), the error in CC3 can easily reach 1 eV, while it goes down to a few tenths of an electronvolt for more common transitions (such as in *trans*-butadiene) involving a significant amount of singles. As expected, CC approaches including quadruples yield highly accurate results for any type of transition. The quality of the excitation energies obtained with multiconfigurational methods is harder to predict. We have found that the overall accuracy of these methods is highly dependent on both the system and the selected active space. The inclusion of the σ and σ^* orbitals in the active space, even for transitions involving mostly π and π^* orbitals, is mandatory in order to reach high accuracy. A theoretical best estimate (TBE) is reported for each transition. We believe that these reference data will be valuable for future methodological developments aiming at accurately describing double excitations.



I. INTRODUCTION

Within the theoretical and computational quantum chemistry community, the term *double excitation* commonly refers to a state whose configuration interaction (CI) or coupled cluster (CC) expansion includes *significant* coefficients or amplitudes associated with doubly excited Slater determinants, i.e., determinants in which two electrons have been promoted from occupied to virtual orbitals of the chosen *reference* determinant. Obviously, this definition is fairly ambiguous as it is highly dependent on the actual reference Slater determinant, and on the magnitude associated with the term “significant”. Moreover, such a picture of placing electrons in orbitals only really applies to one-electron theories, e.g., Hartree–Fock¹ or Kohn–Sham.² In contrast, in a many-electron picture, an excited state is a linear combination of Slater determinants usually built from an intricate mixture of single, double, and higher excitations. In other words, the definition of a double excitation remains fuzzy, and this has led to controversies regarding the nature of the 2^1A_{1g} and 1^1E_{2g} excited states of butadiene^{3–5} and benzene,^{4,5} respectively, to mention two well-known examples.

Although these two states have been classified as doubly excited states in the past, Barca et al. have argued that they can be seen as singly excited states if one allows sufficient orbital relaxation in the excited state.^{4,5} Nonetheless, in the remainder of this work, we will follow one of the common definitions and define a double excitation as an excited state with a significant amount of double-excitation character in the multideterminant expansion.

Double excitations do play a significant role in the proper description of several key physical, chemical, and biological processes, e.g., in photovoltaic devices,⁶ in the photophysics of vision,⁷ and in photochemistry in general^{8–14} involving ubiquitous conical intersections.¹⁵ The second example is intimately linked to the correct location of the excited states of polyenes^{16–28} that are closely related to rhodopsin, which is involved in visual phototransduction.^{29–37} Though doubly excited states do not appear directly in photoabsorption spectra,

Received: November 30, 2018

Published: January 28, 2019

these dark states strongly mix with the bright singly excited states leading to the formation of satellite peaks.^{38,39}

From a theoretical point of view, double excitations are notoriously difficult to model using conventional single-reference methods.⁴⁰ For example, the adiabatic approximation of time-dependent density functional theory (TD-DFT)⁴¹ yields reliable excitation spectra with great efficiency in many cases. Nevertheless, fundamental deficiencies in TD-DFT have been reported for the computation of extended conjugated systems,^{42,43} charge-transfer states,^{44–47} Rydberg states,^{43,48–51} conical intersections,^{15,52} and, more importantly here, for states with double-excitation character.^{15,39,49} Although using range-separated hybrids^{53,54} provides an effective solution to the first three cases, one must go beyond the ubiquitous adiabatic approximation to capture the latter two. (However, this is only true for some types of charge-transfer excitations, as recently discussed by Maitra.⁵⁵) One possible solution is provided by spin-flip TD-DFT which describes double excitations as single excitations from the lowest triplet state.^{33,56–60} However, major limitations pertain.³³ In order to go beyond the adiabatic approximation, a dressed TD-DFT approach has been proposed by Maitra and co-workers^{20,21} (see also refs 25, 27, 28, 39, and 61). In this approach the exchange–correlation kernel is made frequency dependent,^{62,63} which allows one to treat doubly excited states. Albeit far from being a mature black-box approach, ensemble DFT^{64–67} is another viable alternative currently under active development.^{68–75}

As shown by Watson and Chan,⁷⁶ one can also rely on high-level truncation of the equation-of-motion (EOM) formalism of CC theory in order to capture double excitations.^{40,77} However, in order to provide a satisfactory level of correlation for a doubly excited state, one must, at least, introduce contributions from the triple excitations in the CC expansion. In practice, this is often difficult as the scalings of CC3,^{78,79} CCSDT,⁸⁰ and CCSDTQ⁸¹ are N^7 , N^8 , and N^{10} , respectively (where N is the number of basis functions), obviously limiting the applicability of this strategy to small molecules.

Multiconfigurational methods constitute a more natural class of methods to properly treat double excitations. Among these approaches, one finds complete active space self-consistent field (CASSCF),⁸² its second perturbation-corrected variant (CASPT2),⁸³ and the second-order n -electron valence state perturbation theory (NEVPT2).^{84–86} However, the exponential scaling of such methods with the number of active electrons and orbitals also limits their application to small active spaces in their traditional implementation, although using selected configuration interaction (sCI) as an active-space solver allows one to target much larger active spaces.⁸⁷

Alternatively to CC and multiconfigurational methods, one can also compute transition energies for both singly and doubly excited states using sCI methods,^{88–95} which have recently demonstrated their ability to reach near full CI (FCI) quality energies for small molecules.^{96–118} The idea behind such methods is to avoid the exponential increase of the size of the CI expansion by retaining the most energetically relevant determinants only, thanks to the use of a second-order energetic criterion to select perturbatively determinants in the FCI space.^{99,101,103,105,108,109,111,119}

By systematically increasing the order of the CC expansion, the number of determinants in the sCI expansion as well as the size of the one-electron basis set, some of us have recently defined a reference series of more than 100 very accurate vertical transition energies in 18 small compounds.¹¹⁰ However, this set

is constituted almost exclusively of single excitations. Here, we report accurate reference excitation energies for double excitations obtained with both sCI and multiconfigurational methods for a significant number of small- and medium-size molecules using various diffuse-containing basis sets. Moreover, the accuracy obtained with several coupled cluster approaches including, at least, triple excitations are assessed. We believe that these reference data are particularly valuable for future developments of methods aiming at accurately describing double excitations.

This work is organized as follows. Computational details are reported in section II for EOM-CC (section IIA), multiconfigurational (section IIB), and sCI (section IIC) methods. In section III, we discuss our results for each compound and report a theoretical best estimate (TBE) for each transition. We further discuss the overall performance of the different methods and draw our conclusions in section IV.

II. COMPUTATIONAL DETAILS

All geometries used in the present study are available in the Supporting Information. They have been obtained at the CC3/aug-cc-pVTZ level (except for hexatriene, where the geometry has been optimized at the CCSD(T)/aug-cc-pVTZ level) without applying the frozen-core approximation following the same protocol as in earlier works, where additional details can be found.^{110,120} These geometry optimizations were performed with DALTON¹²¹ or CFOUR.¹²² The so-called %T₁ metric giving the percentage of single excitation calculated at the CC3 level in DALTON is employed to characterize the various states. For all calculations, we use the well-known Pople's 6-31+G(d) (in its "5D" spherical version as implemented by default in MOLPRO and DALTON)¹²³ and Dunning's aug-cc-pVXZ ($X = D, T, \text{ and } Q$)¹²⁴ atomic basis sets. In the following, we employ the AVXZ shorthand notations for Dunning's basis sets.

IIA. Coupled Cluster Calculations. Unless otherwise stated, the CC transition energies¹²⁵ were computed in the frozen-core approximation. Globally, we used DALTON¹²¹ to perform the CC3 calculations,^{78,79} CFOUR¹²² for the CCSDT⁸⁰ calculations, and MRCC¹²⁶ for CCSDT⁸⁰ and CCSDTQ⁸¹ (and higher) calculations. Because CFOUR and MRCC rely on different algorithms to locate excited states, we have interchangeably used these two softwares for the CCSDT calculations depending on the targeted transition. Default program settings were generally applied, and when modified, they have been tightened. Note that transition energies are identical in the EOM and linear response (LR) CC formalisms. Consequently, for the sake of brevity, we do not specify the EOM and LR terms in the remaining of this study. The total energies of all CC calculations are available in the Supporting Information.

IIB. Multiconfigurational Calculations. State-averaged (SA) CASSCF and CASPT2^{82,83} have been performed with MOLPRO (RS2 contraction level).¹²⁷ Concerning the NEVPT2 calculations, the partially contracted (PC) and strongly contracted (SC) variants have been systematically tested.^{84–86} From a strict theoretical point of view, we point out that PC-NEVPT2 is supposed to be more accurate than SC-NEVPT2 given that it has a larger number of perturbers and greater flexibility. Additional information and technical details about the CASSCF (as well as CASSCF excitation energies), CASPT2, and NEVPT2 calculations can be found in the Supporting Information. When there is a strong mixing between states with the same spin and spatial symmetries, we have also

performed calculations with multistate (MS) CASPT2 (MS-MR formalism)¹²⁸ and its extended variant (XMS-CASPT2).¹²⁹ Unless otherwise stated, all CASPT2 calculations have been performed with level shift and IPEA parameters set to the standard values of 0.3 and 0.25 au, respectively.

IIC. Selected Configuration Interaction Calculations.

The sCI calculations reported here employ the CIPSI (configuration interaction using a perturbative selection made iteratively)^{90,91,99} algorithm. We refer the interested reader to refs 108–111 and 130 for more details about sCI methods, and the CIPSI algorithm in particular.

In order to treat the electronic states on equal footing, a common set of determinants is selected for the ground state and excited states. These calculations can then be classified as “state-averaged” sCI. Moreover, to speed up convergence to the FCI limit, a common set of natural orbitals issued from a preliminary sCI calculation is employed. For the largest systems, few iterations might be required to obtain a well-behaved convergence of the excitation energies with respect to the number of determinants. For a given atomic basis set, we estimate the FCI limit by linearly extrapolating the sCI energy E_{sCI} as a function of the second-order perturbative correction, E_{PT2} , which is an estimate of the truncation error in the sCI algorithm, i.e., $E_{\text{PT2}} \approx E_{\text{FCI}} - E_{\text{sCI}}$. When $E_{\text{PT2}} = 0$, the FCI limit has effectively been reached. To provide an estimate of the extrapolation error, we report the energy difference between the excitation energies obtained with two- and three-point linear fits. It is, however, a rough estimate as there is no univocal method to quantitatively measure the extrapolation error. This extrapolation procedure has nevertheless been shown to be robust, even for challenging chemical situations.^{105–111} In the following, these extrapolated sCI results are labeled exFCI. Here, E_{PT2} has been efficiently evaluated with a recently proposed hybrid stochastic–deterministic algorithm.¹⁰² Note that we do not report error bars associated with E_{PT2} because the statistical errors originating from this algorithm are orders of magnitude smaller than the extrapolation errors.

All the sCI calculations have been performed in the frozen-core approximation with the electronic structure software QUANTUM PACKAGE, developed in Toulouse and freely available.¹³¹ For the largest molecules considered here, our sCI wave functions contain up to 2×10^8 determinants, which corresponds to an increase of 2 orders of magnitude compared to our previous study.¹¹⁰ Additional information about the sCI wave functions and excitation energies as well as their extrapolated values can be found in the Supporting Information.

III. RESULTS AND DISCUSSION

The molecules considered in the present set are depicted in Figure 1. Vertical transition energies (in eV) obtained with various methods and basis sets are reported in Table 1, together with the nature of the transition. The percentage of single excitation, %T₁, calculated at the CC3 level, is also reported to assess the amount of double-excitation character. Although most of the double excitations are a complicated mixture of singly and doubly (and higher) excited determinants, we have observed that, overall, the %T₁ values obtained at the CC3 level provide a qualitative picture similar to that of the weights of the CI and multiconfigurational wave functions. Reference values taken from the literature are also reported when available. Total energies for each state and additional information as well as CASSCF excitation energies can be found in the Supporting Information. Finally, the error in excitation energies (for a given

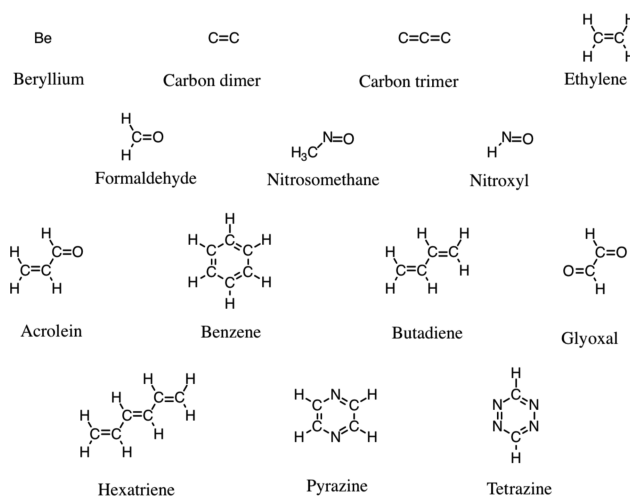


Figure 1. Structure of the various molecules considered in the present set.

atomic basis set and compared to exFCI) for each system is plotted in Figure 2.

IIIA. Beryllium. The beryllium atom (Be) is the smallest system we have considered, and in this specific case, the core electrons have been correlated in all calculations. The lowest double excitation corresponds to the $1s^2 2s^2 (^1S) \rightarrow 1s^2 2p^2 (^1D)$ transition. The %T₁ values which provide an estimate of the weight of the single excitations in the CC3 calculation show that it is mostly a double excitation with a contribution of roughly (only) 30% from the singles.

The energies of the ground and excited states of Be have been computed by Gálves et al.¹³⁴ using explicitly correlated wave functions, and one can extract a value of 7.06 eV for the $1S \rightarrow 1D$ transition from their study. This value is in good agreement with our best estimate of 7.11 eV obtained using the AVQZ basis, the difference being a consequence of the basis set incompleteness. Due to the small number of electrons in Be, exFCI, CCSDT, and CCSDTQ(=FCI) yield identical values for this transition for any of the basis sets considered here. Although slightly different, the CC3 values are close to these reference values with a trifling maximum deviation of 0.02 eV. Irrespective of the method, we note a significant energy difference between the results obtained with People’s 6-31+G(d) basis and the ones obtained with Dunning’s basis sets.

We have also performed multiconfigurational calculations with an active space of 2 electrons in 12 orbitals [CAS(2,12)] constituted by the 2s, 2p, 3p, and 3d orbitals. Due to the diffuse nature of the excited state, it is compulsory to take into account the $n = 3$ shell to reach high accuracy. Excitation energies computed with CASPT2 and NEVPT2 deviate by a maximum of 0.01 eV and are in excellent agreement with the exFCI numbers.

IIIB. Carbon Dimer and Trimer. The second system we discuss is the carbon dimer (C_2), which is a prototype system for strongly correlated and multireference systems.^{141,142} Thanks to its small size, its ground and excited states have been previously scrutinized using highly accurate methods.^{136,143–157} Here, we study two double excitations of different symmetries which are, nonetheless, close in energy: $1^1\Sigma_g^+ \rightarrow 1^1\Delta_g$ and $1^1\Sigma_g^+ \rightarrow 2^1\Sigma_g^+$. These two excitations—both involving excitations from the occupied π_{CC} orbitals to the vacant σ_{CC} orbital—can be classified as “pure” double excitations, as they involve an insignificant amount of single excitations (see Table 1). For the transition $1^1\Sigma_g^+ \rightarrow 2^1\Sigma_g^+$, the theoretical best estimate is most

Table 1. Vertical Transition Energies (eV) for Excited States with Significant Double-Excitation Character in Various Molecules Obtained with Various Methods and Basis Sets^a

molecule	transition	method	basis set				lit.
			6-31+G(d)	AVDZ	AVTZ	AVQZ	
acrolein	$1^1A' \rightarrow 3^1A'$ (π, π) \rightarrow (π^*, π^*)	exFCI	8.00(3)				8.16 ^b
		CC3 (%T ₁)	8.21 (73%)	8.11 (75%)	8.08 (75%)		
		CASPT2	7.93	7.93	7.85	7.84	
		MS-CASPT2	8.36	8.30	8.28	8.30	
		XMS-CASPT2	8.18	8.12	8.07	8.07	
		PC-NEVPT2	7.91	7.93	7.85	7.84	
		SC-NEVPT2	8.08	8.09	8.01	8.00	
benzene	$1^1A_{1g} \rightarrow 1^1E_{2g}$ (π, π) \rightarrow (π^*, π^*)	exFCI	8.40(3)				8.41 ^c
		CCSDT	8.42	8.38			
		CC3 (%T ₁)	8.50 (72%)	8.44 (72%)	8.38 (73%)		
		CASPT2	8.43	8.40	8.34	8.34	
		PC-NEVPT2	8.58	8.56	8.51	8.52	
		SC-NEVPT2	8.62	8.61	8.56	8.56	
	$1^1A_{1g} \rightarrow 2^1A_{1g}$ (π, π) \rightarrow (π^*, π^*)	CASPT2	10.54	10.38	10.28	10.27	10.20 ^d
		MS-CASPT2	11.08	11.00	10.96	10.97	
		XMS-CASPT2	10.77	10.64	10.55	10.54	
		PC-NEVPT2	10.35	10.18	10.00		
		SC-NEVPT2	10.63	10.48	10.38	10.36	
beryllium	$1^1S \rightarrow 1^1D$ ($2s, 2s$) \rightarrow ($2p, 2p$)	exFCI	8.04(0)	7.22(0)	7.15(0)	7.11(0)	7.06 ^e
		CCSDTQ	8.04	7.23	7.15	7.11	
		CCSDT	8.04	7.22	7.15	7.11	
		CC3 (%T ₁)	8.04 (2%)	7.23 (29%)	7.17 (32%)	7.12 (34%)	
		CASPT2	8.02	7.21	7.12	7.10	
		NEVPT2	8.01	7.20	7.11	7.10	
butadiene	$1^1A_g \rightarrow 2^1A_g$ (π, π) \rightarrow (π, π)	exFCI	6.55(3)	6.51(12)			6.55 ^f , 6.39 ^g , 6.58 ^h
		CCSDT	6.63	6.59			
		CC3 (%T ₁)	6.73 (74%)	6.68 (76%)	6.67 (75%)	6.67 (75%)	
		CASPT2	6.80	6.78	6.74	6.75	
		PC-NEVPT2	6.75	6.74	6.70	6.70	
		SC-NEVPT2	6.83	6.82	6.78	6.78	
carbon dimer	$1^1\Sigma_g^+ \rightarrow 1^1\Delta_g$ (π, π) \rightarrow (σ, σ)	exFCI	2.29(0)	2.21(0)	2.09(0)	2.06(0)	2.11 ⁱ
		CCSDTQP	2.29	2.21			
		CCSDTQ	2.32	2.24	2.13		
		CCSDT	2.69	2.63	2.57	2.57	
		CC3 (%T ₁)	3.10 (0%)	3.11 (0%)	3.05 (0%)	3.03 (0%)	
		CASPT2	2.40	2.36	2.24	2.21	
		PC-NEVPT2	2.33	2.26	2.12	2.08	
		SC-NEVPT2	2.35	2.28	2.14	2.11	
	$1^1\Sigma_g^+ \rightarrow 2^1\Sigma_g^+$ (π, π) \rightarrow (σ, σ)	exFCI	2.51(0)	2.50(0)	2.42(0)	2.40(0)	2.43 ⁱ , 2.46 ^j
		CCSDTQP	2.51	2.50			
		CCSDTQ	2.52	2.52	2.45		
		CCSDT	2.86	2.87	2.86	2.87	
		CC3 (%T ₁)	3.23 (0%)	3.28 (0%)	3.26 (0%)	3.24 (0%)	
		CASPT2	2.62	2.65	2.53	2.50	
		PC-NEVPT2	2.54	2.54	2.42	2.39	
		SC-NEVPT2	2.58	2.60	2.48	2.44	
carbon trimer	$1^1\Sigma_g^+ \rightarrow 1^1\Delta_g$ (π, π) \rightarrow (σ, σ)	exFCI	5.27(1)	5.21(0)	5.22(4)	5.23(5)	
		CCSDTQ	5.35	5.31			
		CCSDT	5.85	5.82	5.90	5.92	
		CC3 (%T ₁)	6.65 (0%)	6.65 (0%)	6.68 (1%)	6.66 (1%)	
		CASPT2	5.13	5.06	5.08	5.08	

Table 1. continued

molecule	transition	method	basis set				lit.
			6-31+G(d)	AVDZ	AVTZ	AVQZ	
		PC-NEVPT2	5.26	5.24	5.25	5.26	
		SC-NEVPT2	5.21	5.19	5.21	5.22	
	$1^1\Sigma_g^+ \rightarrow 2^1\Sigma_g^+$ (π, π) \rightarrow (σ, σ)	exFCI	5.93(1)	5.88(0)	5.91(2)	5.86(1)	
		CCSDTQ	6.02	6.00			
		CCSDT	6.52	6.49	6.57	6.58	
		CC3 (%T ₁)	7.20 (1%)	7.20 (1%)	7.24 (1%)	7.22 (1%)	
		CASPT2	5.86	5.81	5.82	5.82	
		PC-NEVPT2	5.97	5.97	5.99	5.99	
		SC-NEVPT2	5.98	5.97	5.99	6.00	
ethylene	$1^1A_g \rightarrow 2^1A_g$	exFCI	13.38(6)	13.07(1)	12.92(6)		12.15 ^k
		CCSDTQ	13.39	13.07			
		CCSDT	13.50	13.20			
		CC3 (%T ₁)	13.82 (4%)	13.57 (15%)	13.42 (20%)	13.06 (61%)	
		CASPT2	13.49	13.23	13.17	13.17	
		MS-CASPT2	13.51	13.26	13.21	13.21	
		XMS-CASPT2	13.50	13.25	13.20	13.20	
		PC-NEVPT2	14.35	13.42	13.11	13.04	
		SC-NEVPT2	13.57	13.33	13.26	13.26	
formaldehyde	$1^1A_1 \rightarrow 3^1A_1$ (n, n) \rightarrow (π^*, π^*)	exFCI	10.86(1)	10.45(1)	10.35(3)		9.82 ^d
		CCSDTQP	10.86				
		CCSDTQ	10.87	10.44			
		CCSDT	11.10	10.78	10.79	10.80	
		CC3 (%T ₁)	11.49 (5%)	11.22 (4%)	11.20 (5%)	11.19 (34%)	
		CASPT2	10.80	10.38	10.27	10.26	
		MS-CASPT2	10.86	10.45	10.35	10.34	
		XMS-CASPT2	10.87	10.47	10.36	10.34	
		PC-NEVPT2	10.84	10.37	10.26	10.25	
		SC-NEVPT2	10.87	10.40	10.30	10.29	
glyoxal	$1^1A_g \rightarrow 2^1A_g$ (n, n) \rightarrow (π^*, π^*)	exFCI	5.60(1)	5.48(0)			5.66 ^l
		CCSDT	6.24	6.22	6.35		
		CC3 (%T ₁)	6.74 (0%)	6.70 (1%)	6.76 (1%)	6.76 (1%)	
		CASPT2	5.58	5.47	5.42	5.43	
		PC-NEVPT2	5.66	5.56	5.52	5.52	
		SC-NEVPT2	5.68	5.58	5.55	5.55	
hexatriene	$1^1A_g \rightarrow 2^1A_g$ (π, π) \rightarrow (π^*, π^*)	CC3 (%T ₁)	5.78 (65%)	5.77 (67%)			5.58 ^h
		CCSDT	5.64	5.65			
		CASPT2	5.62	5.61	5.58	5.58	
		PC-NEVPT2	5.67	5.66	5.64	5.64	
		SC-NEVPT2	5.70	5.69	5.67	5.67	
nitrosomethane	$1^1A' \rightarrow 2^1A'$ (n, n) \rightarrow (π^*, π^*)	exFCI	4.86(1)	4.84(2)	4.76(4)		4.72 ^m
		CCSDT	5.26	5.26	5.29		
		CC3 (%T ₁)	5.73 (2%)	5.75 (4%)	5.76 (3%)	5.74 (2%)	
		CASPT2	4.93	4.88	4.79	4.78	
		PC-NEVPT2	4.92	4.88	4.79	4.78	
		SC-NEVPT2	4.94	4.90	4.81	4.80	
nitroxyl	$1^1A' \rightarrow 2^1A'$ (n, n) \rightarrow (π^*, π^*)	exFCI	4.51(0)	4.40(1)	4.33(0)	4.32(0)	
		CCSDTQP	4.51				
		CCSDTQ	4.54	4.42			
		CCSDT	4.81	4.76	4.79	4.80	
		CC3 (%T ₁)	5.28 (0%)	5.25 (0%)	5.26 (0%)	5.23 (0%)	
		CASPT2	4.55	4.46	4.36	4.34	
		PC-NEVPT2	4.56	4.46	4.37	4.35	

Table 1. continued

molecule	transition	method	basis set				lit.
			6-31+G(d)	AVDZ	AVTZ	AVQZ	
		SC-NEVPT2	4.58	4.48	4.40	4.38	
pyrazine	$1^1A_g \rightarrow 2^1A_g$ (n,n) \rightarrow (π^*,π^*)	CC3 (%T ₁)	9.27 (7%)	9.17 (28%)	9.17 (12%)		
		CASPT2	8.06	7.91	7.81	7.80	
		PC-NEVPT2	8.25	8.12	8.04	8.04	
		SC-NEVPT2	8.27	8.15	8.07	8.07	
	$1^1A_g \rightarrow 3^1A_g$ (π,π) \rightarrow (π^*,π^*)	CC3 (%T ₁)	8.88 (73%)	8.77 (72%)	8.69 (71%)		
		CASPT2	8.91	8.85	8.77	8.77	
		PC-NEVPT2	9.12	9.07	9.00	9.00	
		SC-NEVPT2	9.16	9.12	9.05	9.05	
tetrazine	$1^1A_g \rightarrow 2^1A_g$ (n,n) \rightarrow (π^*,π^*)	CCSDT	5.86	5.86			4.66 ^q
		CC3 (%T ₁)	6.2 2(1%)	6.22 (1%)	6.21 (1%)	6.19 (1%)	
		CASPT2	4.86	4.79	4.69	4.68	
		PC-NEVPT2	4.75	4.70	4.61	4.60	
		SC-NEVPT2	4.82	4.78	4.69	4.68	
	$1^1A_g \rightarrow 1^1B_{3g}$ (n,n) \rightarrow (π_1^*,π_2^*)	CC3 (%T ₁)	7.64 (0%)	7.62 (2%)	7.62 (1%)	7.60 (1%)	5.76 ^o ,6.01 ^r
		CASPT2	6.00	5.95	5.85	5.85	
		PC-NEVPT2	6.25	6.22	6.15	6.14	
		SC-NEVPT2	6.30	6.27	6.20	6.20	
	$1^1A_g \rightarrow 1^3B_{3g}$ (n,n) \rightarrow (π_1^*,π_2^*)	CC3(%T ₁)	7.35(5%)	7.33(5%)	7.35(6%)	7.34(6%)	5.50 ^p
		CASPT2	5.54	5.47	5.39	5.39	
		PC-NEVPT2	5.63	5.58	5.51	5.51	
SC-NEVPT2		5.69	5.64	5.57	5.57		

^a%T₁ is the percentage of single excitation calculated at the CC3 level. For exFCI, an estimate of the extrapolation error is reported in parentheses (not a statistical error bar; see text for details). Values from the literature are provided when available together with their respective reference and level of theory as footnote. ^bReference 132: SAC-CI results using [4s2p1d/2s] + [2s2p2d] basis. ^cReference 133: CC3 results using ANO1 basis (see footnote of Table 5 in ref 133 for more details about the basis set). ^dReference 5: Maximum overlap method (MOM) calculations at the BLYP/cc-pVTZ level. ^eReference 134: Multideterminant explicitly correlated calculations with 17 variational nonlinear parameters in the correlation factor. ^fReference 135: RCA3-F/MR-CISD+Q results with aug'-cc-pVTZ. ^gReference 76: Incremental EOM-CC procedure (up to EOM-CCSDTQ) with CBS extrapolation. ^hReference 107: Heat-bath CI results using AVDZ basis. ⁱReference 136: CEEIS extrapolation procedure (up to sextuple excitations) with CBS extrapolation. ^jReference 106: Heat-bath CI results cc-pV5Z basis. ^kReference 137: MRCISD+Q/SA3-CAS(2,2) results with AVDZ. ^lReference 132: SAC-CI results using [4s2p1d/2s] + [2s2p2d] + [2s2p] basis. ^mReference 110: exFCI/AVTZ data corrected with the difference between CC3/AVQZ and exFCI/AVTZ values. ⁿReference 138: State-specific PC-NEVPT2 results using ANO basis. ^oReference 139: SA-CASSCF/MS-CASPT2 results using AVTZ basis. ^pReference 140: SA-CASSCF/MS-CASPT2 results using TZVP basis.

probably the 2.46 eV value reported by Holmes et al. using the heat-bath CI method and the cc-pV5Z basis set at the experimental geometry.¹⁰⁶ For the $1^1\Sigma_g^+ \rightarrow 1^1\Delta_g$ transition, the value of 2.11 eV obtained by Boschen et al.¹³⁶ (also at the experimental geometry) can be taken as reference. We emphasize that the value for the $1^1\Sigma_g^+ \rightarrow 2^1\Sigma_g^+$ transition taken from this previous investigation is only 0.03 eV from the value reported in ref 106.

The carbon dimer constitutes a nice playground in order to illustrate the convergence of the various methods with respect to the excitation level. For example, we have been able to perform CCSDTQP calculations for the two smallest basis sets, and these results perfectly agree, for each basis set, with the reference exFCI results obtained on the same (CC3) geometry. For all basis sets except the largest one, the CCSDTQ excitation energies are in good agreement with the exFCI results with a maximum deviation of 0.04 eV. With CCSDT, the error compared to exFCI ranges from 0.35 eV up to half an electronvolt, while this error keeps rising for CC3 with a deviation of the order of 0.7–1.0 eV.

Concerning multiconfigurational methods, we have used an active space containing 8 electrons in 8 orbitals [CAS(8,8)], which corresponds to the valence space. NEVPT2 is, by far, the most accurate method with errors below 0.05 eV compared to exFCI. As expected, the partially contracted version of NEVPT2 yields slightly more accurate results compared to its (cheaper) strongly contracted version. CASPT2 excitation energies are consistently higher than exFCI by 0.10–0.15 eV for both transitions. Additional calculations indicate that this bias is due to the IPEA parameter and lowering its value yields substantial improvements. Although CASPT2 is known to generally underestimate excitation energies for single excitations, this rule of thumb does not seem to apply to double excitations.

Due to its relevance in space as well as in terrestrial sooting flames and combustion processes, the carbon trimer C₃ (also known as tricarbon) has motivated numerous theoretical studies.^{158–185} However, its doubly excited states have, to the best of our knowledge, never been studied. Here, we consider the linear geometry which has been found to be the most stable isomer, although the potential energy surface around this minimum is known to be particularly flat.¹⁸⁴

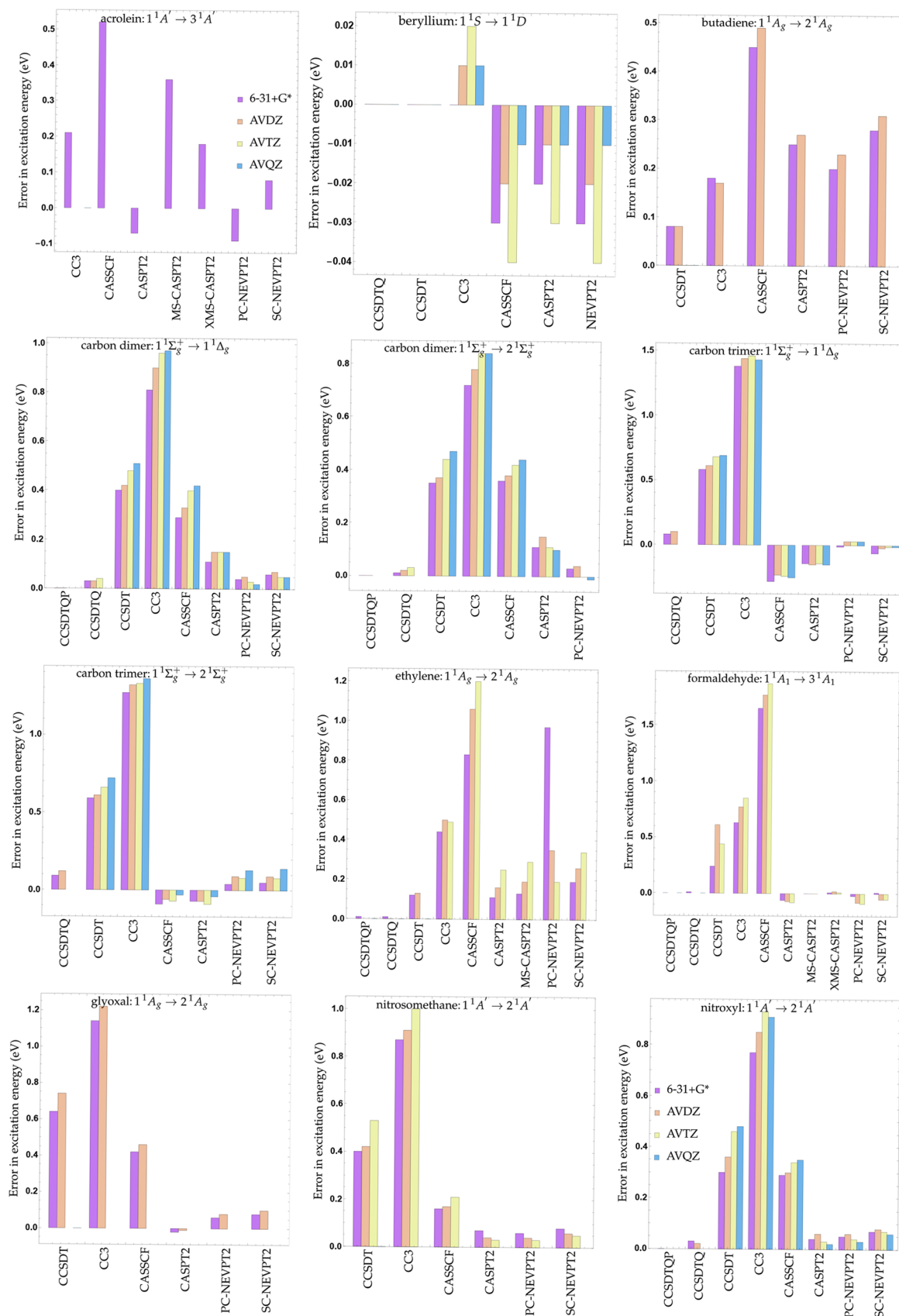


Figure 2. Error in excitation energies (for a given basis and compared to exFCI) for various chemical systems, methods, and basis sets.

Similarly to C_{2v} , we have studied two transitions— $1^1\Sigma_g^+ \rightarrow 1^1\Delta_g$ and $1^1\Sigma_g^+ \rightarrow 2^1\Sigma_g^+$ —which also both involve excitations

from the occupied π_{CC} orbitals to the vacant σ_{CC} orbitals. These lie higher in energy than in the dimer but remain energetically

close to each other. Again, due to the “pure double” nature of the transitions, CC3 very strongly overestimates the reference values (error up to 1.5 eV). Interestingly, CCSDT reduces this error by roughly a factor of 2, bringing the deviation between CCSDT and exFCI in the 0.6–0.7 eV range. This outcome deserves to be highlighted, as, for transitions dominated by single excitations, CC3 and CCSDT have very similar accuracies compared to exFCI.¹¹⁰ Although very expensive, CCSDTQ brings down the error even further to a quite acceptable value of 0.1 eV.

Consistently with C_2 , we have defined a (12,12) active space for the trimer in order to perform multiconfigurational calculations, and we found that the CASPT2 excitation energies are consistently below exFCI by ca. 0.15 eV. Again, NEVPT2 calculations are very accurate with a small preference for SC-NEVPT2, probably due to error compensation.

IIIC. Nitroxyl and Nitrosomethane. Nitroxyl ($H-N=O$) is an important molecule in biochemistry,^{186,187} but only a limited number of theoretical studies of its excited states have been reported to date.^{188–190} For this molecule, the $1^1A' \rightarrow 2^1A'$ transition is a genuine double excitation of the $(n,n) \rightarrow (\pi^*,\pi^*)$ nature. This system is small enough to perform high-order CC calculations, and we have been able to push up to CCSDTQP with the 6-31+G(d) basis. This particular value is in perfect agreement with its exFCI analog in the same basis. For CCSDTQ, we have found that, again, the vertical excitation energies are extremely accurate, with a significant reduction of computational cost compared to CCSDTQP. CCSDT calculations are, as usual, significantly less accurate with an overestimation around 0.3 eV. CC3 adds up to half an electronvolt to this consistent overshooting of the transition energies.

Multiconfigurational calculations have been performed with a (12,9) active space corresponding to the valence space of the nitroso ($-N=O$) fragment. In the case of nitroxyl, NEVPT2 and CASPT2 yield almost identical excitation energies, also very close to the exFCI target.

Nitrosomethane ($CH_3-N=O$) is an interesting test molecule,^{191–194} and it was included in our previous study.¹¹⁰ Similar to nitroxyl, its lowest lying singlet A' excited state corresponds to an almost pure double excitation of $(n,n) \rightarrow (\pi^*,\pi^*)$ nature.¹⁹⁴ Indeed, CC3/AVTZ calculations return a 3% single-excitation character for this transition. Compared to nitroxyl, a clear impact of the methyl group on the double-excitation energy can be noted, but, overall, the same conclusions as in nitroxyl can be drawn for both CC and CAS methods. Therefore, we eschew discussing this case further for the sake of conciseness.

D. Ethylene and Formaldehyde. Despite its small size, ethylene remains a challenging molecule that has received much attention from the theoretical chemistry community^{16,107,140,195–198} and is included in many benchmark sets.^{110,140,199–203} In particular, we refer the interested readers to the work of Davidson and co-workers¹⁹⁸ for what, we believe, is the most complete and accurate investigation dedicated to the excited states of ethylene.

In ethylene, the double-excitation $1^1A_g \rightarrow 2^1A_g$ is of $(\pi,\pi) \rightarrow (\pi^*,\pi^*)$ nature. Unsurprisingly, it has been much less studied than the single excited states due to its fairly high energy and the absence of experimental value. Nevertheless, in 2004, Barbatti et al. reported a value of 12.15 eV at the MRCISD+Q/AVDZ level of theory.¹³⁷ We have found that this state has a fairly high degree of double excitation which, at the CC3 level, decreases

with the size of the basis set, with % T_1 going from 4% with 6-31+G(d) to 61% with AVQZ. Due to its Rydberg character, there is obviously a large basis set effect for this transition, with a magnitude that is additionally strongly method dependent.

Here again, thanks to the small size of this molecule, we have been able to perform high-order CC calculations, and, once more, we have found that CCSDTQP and CCSDTQ yield very accurate excitation energies. Removing the quadruples has the effect of blue-shifting the transition by at least 0.1 eV, while CC3 is off by half an electronvolt independently of the basis set.

In the case of ethylene, we have studied two types of active spaces: a (2,2) active space which includes the π_{CC} and π_{CC}^* orbitals and a (4,4) active space obtained by adding the σ_{CC} and σ_{CC}^* orbitals. Table 1 only reports the results for the largest active space; the values determined with the smaller active space can be found in the Supporting Information. In accordance with previous studies,^{197,198,204} we have found that it is essential to take into account the bonding and antibonding σ orbitals in the active space due to the strong coupling between the σ and π spaces. CASPT2 and NEVPT2 are overestimating the transition energy by at least 0.2 eV with Dunning's bases, while CASPT2 and MS-CASPT2 yield similar excitation energies. We note that the PC-NEVPT2 energies seem to become more accurate when the quality of the atomic basis set improves, whereas the opposite trend is observed for SC-NEVPT2.

From a computational point of view, formaldehyde is similar to ethylene and it has also been extensively studied at various levels of theory.^{110,140,199–203,205–215} However, the $1^1A_1 \rightarrow 3^1A_1$ transition in $CH_2=O$ is rather chemically different from its $H_2C=CH_2$ counterpart, as it is a transition from the ground state to the second excited state of 1^1A_1 symmetry with a $(n,n) \rightarrow (\pi^*,\pi^*)$ character. For this transition, Barca et al.⁴ have reported a value of 9.82 eV at the BLYP/cc-pVTZ level [using the maximum overlap method (MOM) to locate the excited state] in qualitative agreement with our reference energies. The lack of diffuse functions may have, however, a substantial effect on this value.

In terms of the performance of the CC-based methods, the conclusion that we have drawn in ethylene can be almost perfectly transposed to formaldehyde. For the CAS-type calculations, two active spaces were tested: a (4,3) active space that includes the π_{CO} and π_{CO}^* orbitals as well as the lone pair n_O on the oxygen atom, and the (6,5) active space that adds the σ_{CO} and σ_{CO}^* orbitals. Again, Table 1 only reports the results obtained with the largest active space, whereas the values for the smaller active space can be found in the Supporting Information. The performance of multiconfigurational calculations are fairly consistent, and there are no significant differences between the various methods, although, due to the strong mixing between the first three 1^1A_1 states, the results obtained with CASPT2, MS-CASPT2, and XMS-CASPT2 differ slightly. The excitation energies obtained with the multistate variants (extended or not) almost perfectly match the exFCI values, thanks to a small blue shift of the energies compared to the CASPT2 results. Note that the same methods would return excitation energies with errors consistently red-shifted by 0.15 eV with the small active space, highlighting once more that σ orbitals should be included if high accuracy is desired.

E. Butadiene, Glyoxal, and Acrolein. The excited states of (*trans*-)butadiene have been thoroughly studied during the past 30 years.^{3,16,19,21,40,76,107,132,135,196,216–222} In 2012, Watson and Chan⁷⁶ studied the hallmark singlet bright (1^1B_u) and dark (2^1A_g) states. They reported best estimates of 6.21 ± 0.02 and 6.39

± 0.07 eV, respectively, settling down the controversy about the ordering of these two states.²²² While the bright 1B_u state has a clear (HOMO \rightarrow LUMO) single-excitation character, the dark 2A_g state includes a substantial fraction of doubly excited character from the HOMO \rightarrow LUMO double excitation (roughly 30%), yet dominant contributions from the HOMO-1 \rightarrow LUMO and HOMO \rightarrow LUMO+1 single excitations. Butadiene (as well as hexatriene; see below) has been also studied at the dressed TD-DFT level.^{20,21,28}

For butadiene (and the two other molecules considered in this section), exFCI results are only reported for the two double- ζ basis sets, as it was not possible to converge the excitation energies with larger basis sets. Our exFCI estimates agree nicely with the reference values obtained by Dallos and Lischka,¹³⁵ Watson and Chan,⁷⁶ and Chien et al.¹⁰⁷ at the MR-CI, incremental CC, and heat-bath CI levels, respectively (see Table 1).

Concerning the multiconfigurational calculations, the (4,4) active space includes the π_{CC} and π_{CC}^* orbitals, while the (10,10) active space adds the σ_{CC} and σ_{CC}^* orbitals. Expanding the active space has a non-negligible impact on the NEVPT2 excitation energies with a neat improvement by ca. 0.1 eV, whereas CASPT2 results are less sensitive to this active space expansion (see the Supporting Information). As previously mentioned, this effect is reminiscent of the strong coupling between the σ and π spaces in compounds such as butadiene,^{76,223} ethylene,^{197,204} and cyanines.^{111,224–226} Here, it is important to note that both CC3 and CCSDT provide more accurate excitation energies than any multiconfigurational method. This clearly illustrates the strength of CC approaches when there is a dominant “single” nature in the considered transition as discussed in previous works.^{3–5}

The genuine double-excitation $1\ {}^1A_g \rightarrow 2\ {}^1A_g$ in glyoxal,^{132,227–231} which corresponds to a $(n,n) \rightarrow (\pi^*,\pi^*)$ transition, has been studied by Saha et al. at the SAC-CI level¹³² (see Table 1 for additional information). They reported a value of 5.66 eV in very good agreement with our exFCI reference. As expected now, given the “pure” double-excitation character, CC3 and CCSDT are off by the usual margin (more than 1 eV for CC3). Due to the nature of the considered transition, the lone pairs of the two oxygen atoms are included in both the small (8,6) and large (14,12) active spaces. In glyoxal, we have logically found that the lone pairs of both oxygen atoms equally contribute to the double excitation. The (8,6) active space also contains the π_{CC} , π_{CO} , π_{CC}^* , and π_{CO}^* orbitals, while the (14,12) active space adds up the σ_{CC} , σ_{CO} , σ_{CC}^* , and σ_{CO}^* orbitals. CASPT2 excitation energies are particularly close to our exFCI energies, while PC- and SC-NEVPT2 energies are slightly blue-shifted but remain in very good agreement with the exFCI benchmark.

The $1\ {}^1A' \rightarrow 3\ {}^1A'$ excitation in acrolein^{132,232–234} has the same nature as the one in butadiene. However, there is a $1\ {}^1A' \rightarrow 2\ {}^1A'$ transition of $\pi \rightarrow \pi^*$ nature slightly below in energy and these two transitions are strongly coupled. From a computational point of view, it means that the $1\ {}^1A' \rightarrow 3\ {}^1A'$ transition is, from a technical point of view, tricky to get, and this explains why we have not been able to obtain reliable exFCI estimates except for the smallest 6-31+G(d) basis.

The (small) (4,4) active space contains the π_{CC} , π_{CO} , π_{CC}^* , and π_{CO}^* orbitals, while the (larger) (10,10) active space adds up the σ_{CC} , σ_{CO} , σ_{CC}^* , and σ_{CO}^* orbitals. Due to the nature of the transitions involved, it was not necessary to include the lone pair of the oxygen atom in the active space, and this has been

confirmed by preliminary calculations. Moreover, CASSCF predicts the $\pi \rightarrow \pi^*$ transition higher in energy than the $(\pi,\pi) \rightarrow (\pi^*,\pi^*)$ transition, and CASPT2 and NEVPT2 correct this erroneous ordering via the introduction of dynamic correlation. The CAS(4,4) calculations clearly show that the multistate treatment of CASPT2 strongly mix these two transitions, while its extended variant mitigates this trend. Consequently, because of the strong mixing of the three ${}^1A'$ states in acrolein, CASPT2, MS-CASPT2, and XMS-CASPT2 deviate by several tenths of electronvolt.

For the $1\ {}^1A' \rightarrow 3\ {}^1A'$ excitation of acrolein, Saha et al.¹³² provided an estimate of 8.16 eV at the SAC-CI level as compared to our exFCI/6-31+G(d) value of 8.00 eV, which nestles between the PC- and SC-NEVPT2 values. The CC3 excitation energy in the same basis is off by ca. 0.2 eV; so is the XMS-CASPT2 energy.

F. Benzene, Pyrazine, Tetrazine, and Hexatriene. In this last section, we report excitation energies for four larger molecules containing six heavy atoms (see Figure 1). Due to their size, we have not been able to provide reliable exFCI results (except for benzene; see below). Therefore, we mainly restrict ourselves to multiconfigurational calculations with valence π active space as well as CC3 and CCSDT (when technically possible). For the nitrogen-containing molecules, the lone pairs have been included in the active space as we have found that they are always involved in double excitations. We refer the reader to the Supporting Information for details about the active spaces.

Thanks to the high degree of symmetry of benzene, we have been able to obtain a reliable estimate of the excitation energy at the exFCI/6-31+G(d) for the lowest double excitation of $1\ {}^1A_{1g} \rightarrow 1\ {}^1E_{2g}$ character.^{4,5,133,235–244} Our value of 8.40 eV is in almost perfect agreement with the one reported by Christiansen et al.¹³⁵ at the CC3 level (8.41 eV). Indeed, as this particular transition has a rather small double-excitation character, CC3 and CCSDT provide high-quality results. This contrasts with the $1\ {}^1A_{1g} \rightarrow 2\ {}^1A_{1g}$ transition which has almost a pure double-excitation nature. This genuine double excitation has received less attention, but Gill and co-workers reported a value of 10.20 eV at the BLYP(MOM)/cc-pVTZ level in nice agreement with our CASPT2 results. However, we observe that depending on the flavor of post-CASSCF treatment, we have an important variation (by ca. 0.6–0.9 eV) of the excitation energies, the lower and upper bounds being respectively provided by PC-NEVPT2 and MS-CASPT2.

For pyrazine,^{245–250} we have studied the three lowest states of 1A_g symmetry and their corresponding excitation energies. The $1\ {}^1A_g \rightarrow 2\ {}^1A_g$ transition of $(n,n) \rightarrow (\pi^*,\pi^*)$ nature has a large fraction of double excitation, while the $1\ {}^1A_g \rightarrow 3\ {}^1A_g$ transition has a $(\pi,\pi) \rightarrow (\pi^*,\pi^*)$ nature and is dominated by single excitations, similar to the one studied in butadiene and acrolein. In pyrazine, both lone pairs contribute to the second excitation. One can note an interesting methodological inversion between these two transitions. Indeed, due to the contrasted quality of CC3 excitation energies for the $(n,n) \rightarrow (\pi^*,\pi^*)$ and $(\pi,\pi) \rightarrow (\pi^*,\pi^*)$ transitions, the latter is (incorrectly) found below the former at the CC3 level while the opposite is observed with CASPT2 or NEVPT2.

Tetrazine (or *s*-tetrazine)^{140,251–258} is a particularly “rich” molecule in terms of double excitations thanks to the presence of four lone pairs. Here, we have studied three transitions: two singlet–singlet and one singlet–triplet excitations. In these three transitions, electrons from the nitrogen lone pairs n_N are excited to π^* orbitals. As expected, they can be labeled as

Table 2. Theoretical Best Estimates (TBEs) of Vertical Transition Energies (eV) for Excited States with Significant Double-Excitation Character in Various Molecules (See Table 1 for Details)^a

molecule	transition	reference		correction		TBE
		level R/SB	$\Delta E_{R/SB}$	level C/LB	$\Delta E_{C/LB} - \Delta E_{C/SB}$	
acrolein	$1^1A' \rightarrow 3^1A'$	exFCI/6-31+G(d)	8.00	CC3/AVTZ	-0.13	7.87
benzene	$1^1A_g \rightarrow 1^1E_{2g}$	exFCI/6-31+G(d)	8.40	CC3/AVTZ	-0.12	8.28
	$1^1A_g \rightarrow 2^1A_g$	XMS-CASPT2/AVQZ	10.54			10.54
beryllium	$1^1S \rightarrow 1^1D$	ref 134	7.06			7.06
butadiene	$1^1A_g \rightarrow 2^1A_g$	exFCI/AVDZ	6.51	CC3/AVQZ	-0.01	6.50
carbon dimer	$1^1\Sigma_g^+ \rightarrow 1^1\Delta_g$	exFCI/AVQZ	2.06			2.06
	$1^1\Sigma_g^+ \rightarrow 2^1\Sigma_g^+$	exFCI/AVQZ	2.40			2.40
carbon trimer	$1^1\Sigma_g^+ \rightarrow 1^1\Delta_g$	exFCI/AVQZ	5.23			5.23
	$1^1\Sigma_g^+ \rightarrow 2^1\Sigma_g^+$	exFCI/AVQZ	5.86			5.86
ethylene	$1^1A_g \rightarrow 2^1A_g$	exFCI/AVTZ	12.92	CC3/AVQZ	-0.36	12.56
formaldehyde	$1^1A_1 \rightarrow 3^1A_1$	exFCI/AVTZ	10.35	CC3/AVQZ	-0.01	10.34
glyoxal	$1^1A_g \rightarrow 2^1A_g$	exFCI/AVDZ	5.48	CC3/AVQZ	+0.06	5.54
hexatriene	$1^1A_g \rightarrow 2^1A_g$	CC3/AVDZ	5.77	PC-NEVPT2/AVQZ	-0.02	5.75
nitrosomethane	$1^1A' \rightarrow 2^1A'$	exFCI/AVTZ	4.76	CC3/AVQZ	-0.02	4.74
nitroxyl	$1^1A' \rightarrow 2^1A'$	exFCI/AVQZ	4.32			4.32
pyrazine	$1^1A_g \rightarrow 2^1A_g$	PC-NEVPT2/AVQZ	8.04			8.04
	$1^1A_g \rightarrow 3^1A_g$	CC3/AVTZ	8.69	PC-NEVPT2/AVQZ	+0.00	8.69
tetrazine	$1^1A_g \rightarrow 2^1A_g$	PC-NEVPT2/AVQZ	4.60			4.60
	$1^1A_g \rightarrow 1^1B_{3g}$	PC-NEVPT2/AVQZ	6.14			6.14
	$1^1A_g \rightarrow 1^3B_{3g}$	PC-NEVPT2/AVQZ	5.51			5.51

^aTBEs are computed as $\Delta E_{R/SB} + \Delta E_{C/LB} - \Delta E_{C/SB}$, where $\Delta E_{R/SB}$ is the excitation energy computed with a reference (R) method in a small basis (SB), and $\Delta E_{C/SB}$ and $\Delta E_{C/LB}$ are excitation energies computed with a correction (C) method in the small and large basis (LB), respectively.

genuine double excitations as they have very small %T₁ values. For the $1^1A_g \rightarrow 1^1B_{3g}$ and $1^1A_g \rightarrow 1^3B_{3g}$ transitions, we note that the two excited electrons end up in different π^* orbitals, contrary to most cases encountered in the present study. The basis set effect is pretty much inexistent for these three excitations with a maximum difference of 0.04 eV between the smallest and the largest basis sets. For tetrazine, previous high-accuracy reference values are (i) 4.66 eV for the $1^1A_g \rightarrow 2^1A_g$ transition reported by Angeli et al.¹³⁸ with NEVPT2, (ii) 5.76 eV for the $1^1A_g \rightarrow 1^1B_{3g}$ transition reported by Silva-Junior et al.¹³⁹ at the MS-CASPT2/AVTZ level, and (iii) 5.50 eV for the $1^1A_g \rightarrow 1^3B_{3g}$ transition reported by Schreiber et al.¹⁴⁰ at the MS-CASPT2/TZVP level. In comparison, for the second transition, Angeli et al.¹³⁸ have obtained a value of 6.01 eV at the NEVPT2 level. For the first transition, the CCSDT results indicate that the CC3 excitation energies are, again, fairly inaccurate and pushing up to CCSDT does not seem to significantly improve the results as the deviations between CCSDT and CASPT2/NEVPT2 results are still substantial. However, it is hard to determine which method is the most reliable in this case. Finally, we note that, for the second and third transitions, there is an important gap between CASPT2 and NEVPT2 energies.

For hexatriene,^{16,20,21,259,260} the accurate energy of the 2^1A_g state is not known experimentally, illustrating the difficulty to observe these states via conventional spectroscopy techniques. For this molecule, we have unfortunately not been able to provide reliable exFCI results, even for the smallest basis sets. However, Chien et al. have recently reported a value of 5.58 eV at the heat-bath CI/AVDZ level with a MP2/cc-pVQZ geometry.¹⁰⁷ This reference value indicates that our CASPT2 and NEVPT2 calculations are particularly accurate even with a minimal valence π active space, the coupling between σ and π spaces becoming weaker for larger polyenes.¹¹¹ Because the $1^1A_g \rightarrow 2^1A_g$ transition is of $(\pi, \pi) \rightarrow (\pi^*, \pi^*)$ nature (and very

similar to its butadiene analog), the CC3 transition energies are not far off the reference values.

G. Theoretical Best Estimates. In Table 2, we report TBEs for the vertical excitations considered in Table 1. These TBEs are computed as $\Delta E_{R/SB} + \Delta E_{C/LB} - \Delta E_{C/SB}$, where $\Delta E_{R/SB}$ is the excitation energy computed with a reference (R) method in a small basis (SB), and $\Delta E_{C/SB}$ and $\Delta E_{C/LB}$ are excitation energies computed with a correction (C) method in the small and large basis (LB), respectively. By default, we have taken as reference the exFCI excitation energies ($\Delta E_{R/SB}$) computed in the present study, while the basis set correction ($\Delta E_{C/LB} - \Delta E_{C/SB}$) is calculated at the CC3 level. When the exFCI result is unavailable, we have selected, for each excitation separately, what we believe is the most reliable reference method. For most excitations (except the $1^1A_g \rightarrow 2^1A_g$ transition in ethylene), the basis set correction is small. In the case of Be, the value of ref 134 is indisputably more accurate than ours. For C₂, butadiene, and hexatriene, we have not chosen the heat-bath CI results^{106,107} as reference because these calculations were not performed at the same CC3 geometry. However, these values are certainly outstanding references for their corresponding geometry.

IV. CONCLUSION

We have reported reference vertical excitation energies for 20 transitions with significant double-excitation character in a set of 14 small- and medium-size compounds using a series of increasingly large diffuse-containing atomic basis sets (from Pople's 6-31+G(d) to Dunning's aug-cc-pVQZ basis). Depending on the size of the molecule, selected configuration interaction (sCI) and/or multiconfigurational (CASSCF, CASPT2, (X)MS-CASPT2, and NEVPT2) calculations have been performed in order to obtain reliable estimates of the vertical transition energies.

We have shown that the error obtained with CC methods including iterative triples can significantly vary with the exact

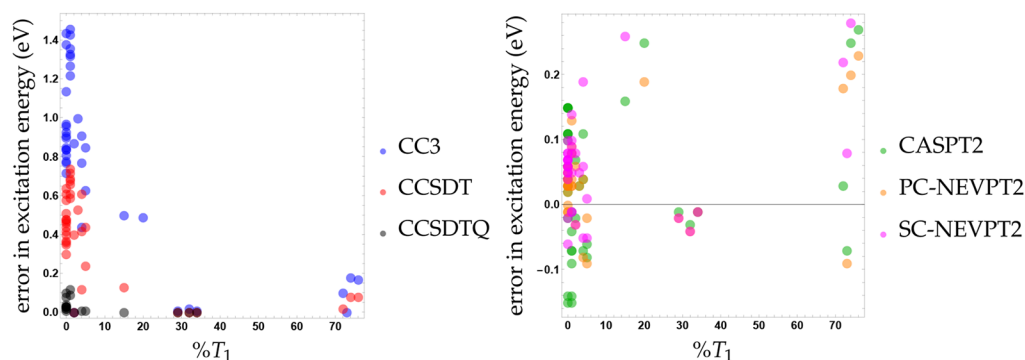


Figure 3. Error in excitation energies (eV) with respect to exFCI as a function of the percentage of single excitation $\%T_1$ (computed at the CC3 level) for various molecules and basis sets. Left: CC3 (blue), CCSDT (red), and CCSDTQ (black). Right: CASPT2 (green), PC-NEVPT2 (orange), and SC-NEVPT2 (pink). Note the difference in scaling of the vertical axes.

nature of the transition. For “pure” double excitations (i.e., for transitions which do not mix with single excitations), the error in CC3 can easily reach 1 eV (and up to 1.5 eV), while it goes down to a few tenths of an electrovolt for more common transitions (such as in butadiene, acrolein, and benzene) involving a significant amount of singles. This analysis is corroborated by Figure 3 which reports the CC3, CCSDT, and CCSDTQ excitation energy errors with respect to exFCI as a function of the percentage of single-excitation $\%T_1$ (computed at the CC3 level). A statistical analysis of these data is also provided in Table 3, where one can find the mean absolute error (MAE) and root-mean-square error (RMSE), as well as the minimum and maximum absolute errors associated with the CC3, CCSDT, and CCSDTQ excitation energies. For CC3, one can see a clear

Table 3. Mean Absolute Error (MAE), Root-Mean-Square Error (RMSE), and Minimum (min) and Maximum (max) Absolute Errors (with Respect to exFCI) of CC3, CCSDT, CCSDTQ, CASPT2, PC-NEVPT2, and SC-NEVPT2 Excitation Energies^a

method	count	MAE	RMSE	min	max
All Excitations					
CC3	39	0.78	0.90	0.00	1.46
CCSDT	37	0.40	0.46	0.00	0.74
CCSDTQ	19	0.03	0.05	0.00	0.12
CASPT2	39	0.03	0.11	0.01	0.27
PC-NEVPT2	39	0.07	0.18	0.00	0.97
SC-NEVPT2	39	0.07	0.12	0.01	0.34
Excitations with $\%T_1 > 50\%$					
CC3	4	0.11	0.13	0.00	0.18
CCSDT	3	0.06	0.07	0.00	0.08
CCSDTQ	0	—	—	—	—
CASPT2	4	0.12	0.19	0.03	0.27
PC-NEVPT2	4	0.13	0.18	0.18	0.23
SC-NEVPT2	4	0.22	0.24	0.08	0.31
Excitations with $\%T_1 < 50\%$					
CC3	35	0.86	0.95	0.00	1.46
CCSDT	34	0.42	0.48	0.00	0.74
CCSDTQ	19	0.03	0.05	0.00	0.12
CASPT2	35	0.02	0.10	0.01	0.25
PC-NEVPT2	35	0.07	0.18	0.00	0.97
SC-NEVPT2	35	0.06	0.10	0.01	0.34

^aAll quantities are given in electrovolt. “Count” refers to the number of transitions considered for each method.

correlation between the magnitude of the error and the degree of double excitation of the corresponding transition. CC3 returns an overall MAE of 0.78 eV, which drops to 0.11 eV when one considers solely excitations with $\%T_1 > 50\%$ (with a maximum error as small as 0.18 eV), but raises to 0.86 eV for excitations with $\%T_1 < 50\%$. Therefore, one can conclude that CC3 is a particularly accurate method for excitations dominated by single excitations which are ubiquitous, for instance, in compounds such as butadiene, acrolein, hexatriene, and benzene derivatives. Indeed, according to our results, CC3 outperforms CASPT2, and NEVPT2 for these transitions (see below). This corroborates the conclusions drawn in our previous investigation where we evidenced that CC3 delivers very small errors with respect to FCI estimates for small compounds.¹¹⁰ A similar trend is observed with CCSDT at a lower scale: the overall MAE is 0.40 eV (a 2-fold reduction compared to CC3), but 0.06 and 0.42 eV for transitions with $\%T_1 > 50\%$ and $\%T_1 < 50\%$, respectively. As expected, more computationally demanding approaches such as CCSDTQ (and beyond) yield highly accurate results even for genuine double excitations. For CCSDTQ, we have not been able to perform calculations on single-dominant excitations as excitations of such type do not seem to appear in small molecules. From a general point of view, CC methods consistently overestimate excitation energies compared to exFCI.

The quality of the excitation energies obtained with multiconfigurational methods such as CASPT2, (X)MS-CASPT2, and NEVPT2 is harder to predict. We have found that the overall accuracy of these methods is highly dependent on the system and the selected active space. Note, however, that including the σ and σ^* orbitals in the active space, even for transitions involving mostly π and π^* orbitals, can significantly improve the excitation energies. The statistics associated with the CASPT2, PC-NEVPT2, and SC-NEVPT2 data are also provided in Table 3 and depicted in Figure 3. The overall MAE of CASPT2 is 0.03 eV, i.e., identical to CCSDTQ, while it is slightly larger for the two NEVPT2 variants (0.07 eV for both of them). However, their RMSE (which gives a bigger weight to large errors) is much larger. Similar observations can be made for excitations with $\%T_1 < 50\%$, while for single-dominant excitations (i.e., $\%T_1 > 50\%$), the MAEs in multiconfigurational methods are higher than in CC-based methods. As a final comment, we note that the consistent overestimation of the exFCI excitation energies observed in CC methods does not apply to multiconfigurational methods.

We believe that the reference data reported in the present study will be particularly valuable for the future development of methods trying to accurately describe double excitations. Although the oscillator strength associated with a double excitation is usually zero or extremely small (dark state), we believe that it would be valuable to study their sensitivity with respect to the level of theory.

■ ASSOCIATED CONTENT

📄 Supporting Information

The Supporting Information is available free of charge on the ACS Publications website at DOI: 10.1021/acs.jctc.8b01205.

Geometries and additional information (including total energies) on the CC, multiconfigurational, and sCI calculations (PDF)

■ AUTHOR INFORMATION

Corresponding Author

*E-mail: loos@irsamc.ups-tlse.fr.

ORCID

Pierre-François Loos: 0000-0003-0598-7425

Martial Boggio-Pasqua: 0000-0001-6684-5223

Denis Jacquemin: 0000-0002-4217-0708

Notes

The authors declare no competing financial interest.

■ ACKNOWLEDGMENTS

P.-F.L. thanks Emmanuel Giner and Jean-Paul Malrieu for NEVPT2-related discussions. P.-F.L. and A.S. thank Nicolas Renon and Pierrette Barbaresco (CALMIP, Toulouse) for technical assistance. D.J. acknowledges the *Région des Pays de la Loire* for financial support. This work was performed using HPC resources from (i) GENCI-TGCC (Grant No. 2018-A0040801738), (ii) CCIPL (*Centre de Calcul Intensif des Pays de Loire*), (iii) the Troy cluster installed in Nantes, and (iv) CALMIP (Toulouse) under allocations 2018-0510, 2018-18005, and 2018-12158.

■ REFERENCES

- (1) Szabo, A.; Ostlund, N. S. *Modern quantum chemistry*; McGraw-Hill: New York, 1989.
- (2) Parr, R. G.; Yang, W. *Density-functional theory of atoms and molecules*; Clarendon Press: Oxford, U.K., 1989.
- (3) Shu, Y.; Truhlar, D. G. Doubly Excited Character or Static Correlation of the Reference State in the Controversial 2^1A_g State of *Trans*-Butadiene? *J. Am. Chem. Soc.* **2017**, *139*, 13770–13778.
- (4) Barca, G. M. J.; Gilbert, A. T. B.; Gill, P. M. W. Simple Models for Difficult Electronic Excitations. *J. Chem. Theory Comput.* **2018**, *14*, 1501–1509.
- (5) Barca, G. M. J.; Gilbert, A. T. B.; Gill, P. M. W. Excitation Number: Characterizing Multiply Excited States. *J. Chem. Theory Comput.* **2018**, *14*, 9–13.
- (6) Delgado, J. L.; Bouit, P.-A.; Filippone, S.; Herranz, M.; Martín, N. Organic Photovoltaics: A Chemical Approach. *Chem. Commun.* **2010**, 46, 4853.
- (7) Palczewski, K. G. Protein–Coupled Receptor Rhodopsin. *Annu. Rev. Biochem.* **2006**, *75*, 743–767.
- (8) Bernardi, F.; De, S.; Olivucci, M.; Robb, M. A. The Mechanism of Ground-State-Forbidden Photochemical Pericyclic Reactions: Evidence for Real Conical Intersections. *J. Am. Chem. Soc.* **1990**, *112*, 1737–1744.
- (9) Bernardi, F.; Olivucci, M.; Robb, M. A. Potential Energy Surface Crossings in Organic Photochemistry. *Chem. Soc. Rev.* **1996**, *25*, 321.
- (10) Boggio-Pasqua, M.; Bearpark, M. J.; Robb, M. A. Toward a Mechanistic Understanding of the Photochromism of Dimethyldihydroxyrenes. *J. Org. Chem.* **2007**, *72*, 4497–4503.
- (11) Klessinger, M.; Michl, J. *Excited States and Photochemistry of Organic Molecules*; VCH: New York, 1995; .
- (12) Olivucci, M. *Computational Photochemistry*; Elsevier Science: Amsterdam, 2010.
- (13) Robb, M. A.; Garavelli, M.; Olivucci, M.; Bernardi, F. A Computational Strategy for Organic Photochemistry. In *Reviews in Computational Chemistry*; Lipkowitz, K. B., Boyd, D. B., Eds.; John Wiley & Sons: Hoboken, NJ, USA, 2000; pp 87–146, DOI: 10.1002/9780470125922.ch2.
- (14) Van der Lugt, W. T. A. M.; Oosterhoff, L. J. Symmetry Control and Photoinduced Reactions. *J. Am. Chem. Soc.* **1969**, *91*, 6042–6049.
- (15) Levine, B. G.; Ko, C.; Quenneville, J.; Martínez, T. J. Conical Intersections and Double Excitations in Time-Dependent Density Functional Theory. *Mol. Phys.* **2006**, *104*, 1039–1051.
- (16) Serrano-Andrés, L.; Merchán, M.; Nebot-Gil, I.; Lindh, R.; Roos, B. O. Towards an Accurate Molecular Orbital Theory for Excited States: Ethene, Butadiene, and Hexatriene. *J. Chem. Phys.* **1993**, *98*, 3151–3162.
- (17) Cave, R. J.; Davidson, E. R. Theoretical Investigation of Several Low-Lying States of *Trans*, *Trans*-1, 3,5-Hexatriene. *J. Phys. Chem.* **1988**, *92*, 614–620.
- (18) Lappe, J.; Cave, R. J. On the Vertical and Adiabatic Excitation Energies of the 2^1A_g State of *Trans* -1,3-Butadiene. *J. Phys. Chem. A* **2000**, *104*, 2294–2300.
- (19) Boggio-Pasqua, M.; Bearpark, M. J.; Klene, M.; Robb, M. A. A Computational Strategy for Geometry Optimization of Ionic and Covalent Excited States, Applied to Butadiene and Hexatriene. *J. Chem. Phys.* **2004**, *120*, 7849–7860.
- (20) Maitra, N. T.; Zhang, F.; Cave, R. J.; Burke, K. Double Excitations within Time-Dependent Density Functional Theory Linear Response. *J. Chem. Phys.* **2004**, *120*, 5932–5937.
- (21) Cave, R. J.; Zhang, F.; Maitra, N. T.; Burke, K. A Dressed TDDFT Treatment of the 2^1A_g States of Butadiene and Hexatriene. *Chem. Phys. Lett.* **2004**, *389*, 39–42.
- (22) Wanko, M.; Hoffmann, M.; Strodel, P.; Koslowski, A.; Thiel, W.; Neese, F.; Frauenheim, T.; Elstner, M. Calculating Absorption Shifts for Retinal Proteins: Computational Challenges. *J. Phys. Chem. B* **2005**, *109*, 3606–3615.
- (23) Starcke, J. H.; Wormit, M.; Schirmer, J.; Dreuw, A. How Much Double Excitation Character Do the Lowest Excited States of Linear Polyenes Have? *Chem. Phys.* **2006**, *329*, 39–49.
- (24) Catalán, J.; de Paz, J. L. G. On the Photophysics of All- *Trans* Polyenes: Hexatriene versus Octatetraene. *J. Chem. Phys.* **2006**, *124*, 034306.
- (25) Mazur, G.; Włodarczyk, R. Application of the Dressed Time-Dependent Density Functional Theory for the Excited States of Linear Polyenes. *J. Comput. Chem.* **2009**, *30*, 811–817.
- (26) Angeli, C. An Analysis of the Dynamic σ Polarization in the V State of Ethene. *Int. J. Quantum Chem.* **2010**, 2436–2447.
- (27) Mazur, G.; Makowski, M.; Włodarczyk, R.; Aoki, Y. Dressed TDDFT Study of Low-Lying Electronic Excited States in Selected Linear Polyenes and Diphenylpolyenes. *Int. J. Quantum Chem.* **2011**, *111*, 819–825.
- (28) Huix-Rotllant, M.; Ipatov, A.; Rubio, A.; Casida, M. E. Assessment of Dressed Time-Dependent Density-Functional Theory for the Low-Lying Valence States of 28 Organic Chromophores. *Chem. Phys.* **2011**, *391*, 120–129.
- (29) Gozem, S.; Huntress, M.; Schapiro, I.; Lindh, R.; Granovsky, A. A.; Angeli, C.; Olivucci, M. Dynamic Electron Correlation Effects on the Ground State Potential Energy Surface of a Retinal Chromophore Model. *J. Chem. Theory Comput.* **2012**, *8*, 4069–4080.
- (30) Gozem, S.; Krylov, A. I.; Olivucci, M. Conical Intersection and Potential Energy Surface Features of a Model Retinal Chromophore: Comparison of EOM-CC and Multireference Methods. *J. Chem. Theory Comput.* **2013**, *9*, 284–292.

- (31) Gozem, S.; Melaccio, F.; Lindh, R.; Krylov, A. I.; Granovsky, A. A.; Angeli, C.; Olivucci, M. Mapping the Excited State Potential Energy Surface of a Retinal Chromophore Model with Multireference and Equation-of-Motion Coupled-Cluster Methods. *J. Chem. Theory Comput.* **2013**, *9*, 4495–4506.
- (32) Gozem, S.; Melaccio, F.; Valentini, A.; Filatov, M.; Huix-Rotllant, M.; Ferré, N.; Frutos, L. M.; Angeli, C.; Krylov, A. I.; Granovsky, A. A.; Lindh, R.; Olivucci, M. Shape of Multireference, Equation-of-Motion Coupled-Cluster, and Density Functional Theory Potential Energy Surfaces at a Conical Intersection. *J. Chem. Theory Comput.* **2014**, *10*, 3074–3084.
- (33) Huix-Rotllant, M.; Natarajan, B.; Ipatov, A.; Muhavini Wawire, C.; Deutsch, T.; Casida, M. E. Assessment of Noncollinear Spin-Flip Tamm–Dancoff Approximation Time-Dependent Density-Functional Theory for the Photochemical Ring-Opening of Oxirane. *Phys. Chem. Chem. Phys.* **2010**, *12*, 12811.
- (34) Xu, X.; Gozem, S.; Olivucci, M.; Truhlar, D. G. Combined Self-Consistent-Field and Spin-Flip Tamm–Dancoff Density Functional Approach to Potential Energy Surfaces for Photochemistry. *J. Phys. Chem. Lett.* **2013**, *4*, 253–258.
- (35) Schapiro, I.; Neese, F. SORCI for Photochemical and Thermal Reaction Paths: A Benchmark Study. *Comput. Theor. Chem.* **2014**, *1040–1041*, 84–98.
- (36) Tuna, D.; Lefrancois, D.; Wolański, L.; Gozem, S.; Schapiro, I.; Andruniów, T.; Dreuw, A.; Olivucci, M. Assessment of Approximate Coupled-Cluster and Algebraic-Diagrammatic-Construction Methods for Ground- and Excited-State Reaction Paths and the Conical-Intersection Seam of a Retinal-Chromophore Model. *J. Chem. Theory Comput.* **2015**, *11*, 5758–5781.
- (37) Manathunga, M.; Yang, X.; Luk, H. L.; Gozem, S.; Frutos, L. M.; Valentini, A.; Ferré, N.; Olivucci, M. Probing the Photodynamics of Rhodopsins with Reduced Retinal Chromophores. *J. Chem. Theory Comput.* **2016**, *12*, 839–850.
- (38) Helbig, N.; Fuks, J.; Tokatly, I.; Appel, H.; Gross, E.; Rubio, A. Time-Dependent Density-Functional and Reduced Density-Matrix Methods for Few Electrons: Exact versus Adiabatic Approximations. *Chem. Phys.* **2011**, *391*, 1–10.
- (39) Elliott, P.; Goldson, S.; Canahui, C.; Maitra, N. T. Perspectives on Double-Excitations in TDDFT. *Chem. Phys.* **2011**, *391*, 110–119.
- (40) Sundstrom, E. J.; Head-Gordon, M. Non-Orthogonal Configuration Interaction for the Calculation of Multielectron Excited States. *J. Chem. Phys.* **2014**, *140*, 114103.
- (41) Casida, M. E. In *Recent Advances in Density Functional Methods*; Chong, D. P., Ed.; World Scientific: Singapore, 1995; p 155, DOI: 10.1142/2914.
- (42) Woodcock, H. L.; Schaefer, H. F.; Schreiner, P. R. Problematic Energy Differences between Cumulenes and Poly-Ynes: Does This Point to a Systematic Improvement of Density Functional Theory? *J. Phys. Chem. A* **2002**, *106*, 11923–11931.
- (43) Tozer, D. J. Relationship between Long-Range Charge-Transfer Excitation Energy Error and Integer Discontinuity in Kohn–Sham Theory. *J. Chem. Phys.* **2003**, *119*, 12697–12699.
- (44) Tozer, D. J.; Amos, R. D.; Handy, N. C.; Roos, B. O.; Serrano-Andrés, L. Does Density Functional Theory Contribute to the Understanding of Excited States of Unsaturated Organic Compounds? *Mol. Phys.* **1999**, *97*, 859–868.
- (45) Dreuw, A.; Weisman, J. L.; Head-Gordon, M. Long-Range Charge-Transfer Excited States in Time-Dependent Density Functional Theory Require Non-Local Exchange. *J. Chem. Phys.* **2003**, *119*, 2943–2946.
- (46) Sobolewski, A. L.; Domcke, W. Ab Initio Study of the Excited-State Coupled Electron–Proton-Transfer Process in the 2-Aminopyridine Dimer. *Chem. Phys.* **2003**, *294*, 73–83.
- (47) Dreuw, A.; Head-Gordon, M. Failure of Time-Dependent Density Functional Theory for Long-Range Charge-Transfer Excited States: The Zincbacteriochlorin-Bacteriochlorin and Bacteriochlorophyll-Spheroidene Complexes. *J. Am. Chem. Soc.* **2004**, *126*, 4007–4016.
- (48) Tozer, D. J.; Handy, N. C. Improving Virtual Kohn–Sham Orbitals and Eigenvalues: Application to Excitation Energies and Static Polarizabilities. *J. Chem. Phys.* **1998**, *109*, 10180–10189.
- (49) Tozer, D. J.; Handy, N. C. On the Determination of Excitation Energies Using Density Functional Theory. *Phys. Chem. Chem. Phys.* **2000**, *2*, 2117–2121.
- (50) Casida, M. E.; Jamorski, C.; Casida, K. C.; Salahub, D. R. Molecular Excitation Energies to High-Lying Bound States from Time-Dependent Density-Functional Response Theory: Characterization and Correction of the Time-Dependent Local Density Approximation Ionization Threshold. *J. Chem. Phys.* **1998**, *108*, 4439–4449.
- (51) Casida, M. E.; Salahub, D. R. Asymptotic Correction Approach to Improving Approximate Exchange–Correlation Potentials: Time-Dependent Density-Functional Theory Calculations of Molecular Excitation Spectra. *J. Chem. Phys.* **2000**, *113*, 8918–8935.
- (52) Tapavicza, E.; Tavernelli, I.; Rothlisberger, U.; Filippi, C.; Casida, M. E. Mixed Time-Dependent Density-Functional Theory/Classical Trajectory Surface Hopping Study of Oxirane Photochemistry. *J. Chem. Phys.* **2008**, *129*, 124108.
- (53) Tawada, Y.; Tsuneda, T.; Yanagisawa, S.; Yanai, T.; Hirao, K. A Long-Range-Corrected Time-Dependent Density Functional Theory. *J. Chem. Phys.* **2004**, *120*, 8425–8433.
- (54) Yanai, T.; Tew, D. P.; Handy, N. C. A New Hybrid Exchange–Correlation Functional Using the Coulomb-Attenuating Method (CAM-B3LYP). *Chem. Phys. Lett.* **2004**, *393*, 51–57.
- (55) Maitra, N. T. Charge Transfer in Time-Dependent Density Functional Theory. *J. Phys.: Condens. Matter* **2017**, *29*, 423001.
- (56) Krylov, A. I. Spin-Flip Configuration Interaction: An Electronic Structure Model That Is Both Variational and Size-Consistent. *Chem. Phys. Lett.* **2001**, *350*, 522–530.
- (57) Shao, Y.; Head-Gordon, M.; Krylov, A. I. The Spin–Flip Approach within Time-Dependent Density Functional Theory: Theory and Applications to Diradicals. *J. Chem. Phys.* **2003**, *118*, 4807–4818.
- (58) Wang, F.; Ziegler, T. Time-Dependent Density Functional Theory Based on a Noncollinear Formulation of the Exchange–Correlation Potential. *J. Chem. Phys.* **2004**, *121*, 12191.
- (59) Wang, F.; Ziegler, T. Use of Noncollinear Exchange–Correlation Potentials in Multiplet Resolutions by Time-Dependent Density Functional Theory. *Int. J. Quantum Chem.* **2006**, *106*, 2545–2550.
- (60) Minezawa, N.; Gordon, M. S. Optimizing Conical Intersections by Spin-Flip Density Functional Theory: Application to Ethylene. *J. Phys. Chem. A* **2009**, *113*, 12749–12753.
- (61) Maitra, N. T. Memory: History, Initial-State Dependence, and Double-Excitations. In *Fundamentals of Time-Dependent Density Functional Theory*; Marques, M. A., Maitra, N. T., Nogueira, F. M., Gross, E., Rubio, A., Eds.; Springer: Berlin, Heidelberg, 2012; Vol. 837, pp 167–184, DOI: 10.1007/978-3-642-23518-4_8.
- (62) Romaniello, P.; Sangalli, D.; Berger, J. A.; Sottile, F.; Molinari, L. G.; Reining, L.; Onida, G. Double Excitations in Finite Systems. *J. Chem. Phys.* **2009**, *130*, 044108.
- (63) Sangalli, D.; Romaniello, P.; Onida, G.; Marini, A. Double Excitations in Correlated Systems: A Many–Body Approach. *J. Chem. Phys.* **2011**, *134*, 034115.
- (64) Theophilou, A. K. The Energy Density Functional Formalism for Excited States. *J. Phys. C: Solid State Phys.* **1979**, *12*, 5419–5430.
- (65) Gross, E. K. U.; Oliveira, L. N.; Kohn, W. Density-Functional Theory for Ensembles of Fractionally Occupied States. I. Basic Formalism. *Phys. Rev. A: At, Mol., Opt. Phys.* **1988**, *37*, 2809–2820.
- (66) Gross, E. K. U.; Oliveira, L. N.; Kohn, W. Rayleigh-Ritz Variational Principle for Ensembles of Fractionally Occupied States. *Phys. Rev. A: At, Mol., Opt. Phys.* **1988**, *37*, 2805–2808.
- (67) Oliveira, L. N.; Gross, E. K. U.; Kohn, W. Density-Functional Theory for Ensembles of Fractionally Occupied States. II. Application to the He Atom. *Phys. Rev. A: At, Mol., Opt. Phys.* **1988**, *37*, 2821–2833.
- (68) Kazaryan, A.; Heuver, J.; Filatov, M. Excitation Energies from Spin-Restricted Ensemble-Referenced Kohn–Sham Method: A State-Average Approach. *J. Phys. Chem. A* **2008**, *112*, 12980–12988.
- (69) Filatov, M.; Huix-Rotllant, M.; Burghardt, I. Ensemble Density Functional Theory Method Correctly Describes Bond Dissociation,

Excited State Electron Transfer, and Double Excitations. *J. Chem. Phys.* **2015**, *142*, 184104.

(70) Senjean, B.; Knecht, S.; Jensen, H. J. A.; Fromager, E. Linear Interpolation Method in Ensemble Kohn-Sham and Range-Separated Density-Functional Approximations for Excited States. *Phys. Rev. A: At, Mol., Opt. Phys.* **2015**, *92*, 012518.

(71) Filatov, M. Ensemble DFT Approach to Excited States of Strongly Correlated Molecular Systems. In *Density-Functional Methods for Excited States*; Ferré, N., Filatov, M., Huix-Rotllant, M., Eds.; Springer: Cham, Switzerland, 2015; Vol. 368, pp 97–124.

(72) Filatov, M. Spin-Restricted Ensemble-Referenced Kohn-Sham Method: Basic Principles and Application to Strongly Correlated Ground and Excited States of Molecules. *WIREs Comput. Mol. Sci.* **2015**, *5*, 146–167.

(73) Deur, K.; Mazouin, L.; Fromager, E. Exact Ensemble Density Functional Theory for Excited States in a Model System: Investigating the Weight Dependence of the Correlation Energy. *Phys. Rev. B: Condens. Matter Mater. Phys.* **2017**, *95*, 035120.

(74) Gould, T.; Kronik, L.; Pittalis, S. Charge Transfer Excitations from Exact and Approximate Ensemble Kohn-Sham Theory. *J. Chem. Phys.* **2018**, *148*, 174101.

(75) Sagredo, F.; Burke, K. Accurate Double Excitations from Ensemble Density Functional Calculations. *J. Chem. Phys.* **2018**, *149*, 134103.

(76) Watson, M. A.; Chan, G. K.-L. Excited States of Butadiene to Chemical Accuracy: Reconciling Theory and Experiment. *J. Chem. Theory Comput.* **2012**, *8*, 4013–4018.

(77) Hirata, S.; Nooijen, M.; Bartlett, R. J. High-Order Determinantal Equation-of-Motion Coupled-Cluster Calculations for Electronic Excited States. *Chem. Phys. Lett.* **2000**, *326*, 255–262.

(78) Christiansen, O.; Koch, H.; Jørgensen, P. Response Functions in the CC3 Iterative Triple Excitation Model. *J. Chem. Phys.* **1995**, *103*, 7429–7441.

(79) Koch, H.; Christiansen, O.; Jørgensen, P.; Sanchez de Merás, A. M.; Helgaker, T. The CC3Model: An Iterative Coupled Cluster Approach Including Connected Triples. *J. Chem. Phys.* **1997**, *106*, 1808–1818.

(80) Noga, J.; Bartlett, R. J. The Full CCSDT Model for Molecular Electronic Structure. *J. Chem. Phys.* **1987**, *86*, 7041–7050.

(81) Kucharski, S. A.; Bartlett, R. J. Recursive Intermediate Factorization and Complete Computational Linearization of the Coupled-Cluster Single, Double, Triple, and Quadruple Excitation Equations. *Theor. Chim. Acta* **1991**, *80*, 387–405.

(82) Roos, B. O.; Andersson, K.; Fulscher, M. P.; Malmqvist, P.-A.; Serrano-Andrés, L. In *Advances in Chemical Physics*; Prigogine, I., Rice, S. A., Eds.; Wiley: New York, 1996; Vol. XCIII, pp 219–331.

(83) Andersson, K.; Malmqvist, P. A.; Roos, B. O.; Sadlej, A. J.; Wolinski, K. Second-Order Perturbation Theory With a CASSCF Reference Function. *J. Phys. Chem.* **1990**, *94*, 5483–5488.

(84) Angeli, C.; Cimiraglia, R.; Malrieu, J.-P. N-Electron Valence State Perturbation Theory: A Fast Implementation of the Strongly Contracted Variant. *Chem. Phys. Lett.* **2001**, *350*, 297–305.

(85) Angeli, C.; Cimiraglia, R.; Evangelisti, S.; Leininger, T.; Malrieu, J.-P. Introduction of n -Electron Valence States for Multireference Perturbation Theory. *J. Chem. Phys.* **2001**, *114*, 10252–10264.

(86) Angeli, C.; Cimiraglia, R.; Malrieu, J.-P. N-Electron Valence State Perturbation Theory: A Spinless Formulation and an Efficient Implementation of the Strongly Contracted and of the Partially Contracted Variants. *J. Chem. Phys.* **2002**, *117*, 9138–9153.

(87) Smith, J. E. T.; Mussard, B.; Holmes, A. A.; Sharma, S. Cheap and Near Exact CASSCF with Large Active Spaces. *J. Chem. Theory Comput.* **2017**, *13*, 5468–5478.

(88) Bender, C. F.; Davidson, E. R. Studies in Configuration Interaction: The First-Row Diatomic Hydrides. *Phys. Rev.* **1969**, *183*, 23–30.

(89) Whitten, J. L.; Hackmeyer, M. Configuration Interaction Studies of Ground and Excited States of Polyatomic Molecules. I. The CI Formulation and Studies of Formaldehyde. *J. Chem. Phys.* **1969**, *51*, 5584–5596.

(90) Huron, B.; Malrieu, J. P.; Rancurel, P. Iterative perturbation calculations of ground and excited state energies from multiconfigurational zeroth-order wavefunctions. *J. Chem. Phys.* **1973**, *58*, 5745–5759.

(91) Evangelisti, S.; Daudey, J.-P.; Malrieu, J.-P. Convergence of an improved CIPSI algorithm. *Chem. Phys.* **1983**, *75*, 91–102.

(92) Cimiraglia, R. Second order perturbation correction to CI energies by use of diagrammatic techniques: An improvement to the CIPSI algorithm. *J. Chem. Phys.* **1985**, *83*, 1746–1749.

(93) Cimiraglia, R.; Persico, M. Recent advances in multireference second order perturbation CI: The CIPSI method revisited. *J. Comput. Chem.* **1987**, *8*, 39–47.

(94) Illas, F.; Rubio, J.; Ricart, J. M. Approximate natural orbitals and the convergence of a second order multireference many-body perturbation theory (CIPSI) algorithm. *J. Chem. Phys.* **1988**, *89*, 6376–6384.

(95) Povill, A.; Rubio, J.; Illas, F. Treating large intermediate spaces in the CIPSI method through a direct selected CI algorithm. *Theor. Chem. Acc.* **1992**, *82*, 229–238.

(96) Abrams, M. L.; Sherrill, C. D. Important configurations in configuration interaction and coupled-cluster wave functions. *Chem. Phys. Lett.* **2005**, *412*, 121–124.

(97) Bunge, C. F.; Carbó-Dorca, R. Select-divide-and-conquer method for large-scale configuration interaction. *J. Chem. Phys.* **2006**, *125*, 014108.

(98) Bytautas, L.; Ruedenberg, K. A priori identification of configurational deadwood. *Chem. Phys.* **2009**, *356*, 64–75.

(99) Giner, E.; Scemama, A.; Caffarel, M. Using perturbatively selected configuration interaction in quantum Monte Carlo calculations. *Can. J. Chem.* **2013**, *91*, 879–885.

(100) Caffarel, M.; Giner, E.; Scemama, A.; Ramírez-Solís, A. Spin Density Distribution in Open-Shell Transition Metal Systems: A Comparative Post-Hartree–Fock, Density Functional Theory, and Quantum Monte Carlo Study of the CuCl₂ Molecule. *J. Chem. Theory Comput.* **2014**, *10*, 5286–5296.

(101) Giner, E.; Scemama, A.; Caffarel, M. Fixed-node diffusion Monte Carlo potential energy curve of the fluorine molecule F₂ using selected configuration interaction trial wavefunctions. *J. Chem. Phys.* **2015**, *142*, 044115.

(102) Garniron, Y.; Scemama, A.; Loos, P.-F.; Caffarel, M. Hybrid stochastic-deterministic calculation of the second-order perturbative contribution of multireference perturbation theory. *J. Chem. Phys.* **2017**, *147*, 034101.

(103) Caffarel, M.; Applencourt, T.; Giner, E.; Scemama, A. Communication: Toward an improved control of the fixed-node error in quantum Monte Carlo: The case of the water molecule. *J. Chem. Phys.* **2016**, *144*, 151103.

(104) Holmes, A. A.; Tubman, N. M.; Umrigar, C. J. Heat-Bath Configuration Interaction: An Efficient Selected Configuration Interaction Algorithm Inspired by Heat-Bath Sampling. *J. Chem. Theory Comput.* **2016**, *12*, 3674–3680.

(105) Sharma, S.; Holmes, A. A.; Jeanmairet, G.; Alavi, A.; Umrigar, C. J. Semistochastic Heat-Bath Configuration Interaction Method: Selected Configuration Interaction with Semistochastic Perturbation Theory. *J. Chem. Theory Comput.* **2017**, *13*, 1595–1604.

(106) Holmes, A. A.; Umrigar, C. J.; Sharma, S. Excited states using semistochastic heat-bath configuration interaction. *J. Chem. Phys.* **2017**, *147*, 164111.

(107) Chien, A. D.; Holmes, A. A.; Otten, M.; Umrigar, C. J.; Sharma, S.; Zimmerman, P. M. Excited States of Methylene, Polyenes, and Ozone from Heat-Bath Configuration Interaction. *J. Phys. Chem. A* **2018**, *122*, 2714–2722.

(108) Scemama, A.; Garniron, Y.; Caffarel, M.; Loos, P. F. Deterministic construction of nodal surfaces within quantum Monte Carlo: the case of FeS. *J. Chem. Theory Comput.* **2018**, *14*, 1395.

(109) Scemama, A.; Benali, A.; Jacquemin, D.; Caffarel, M.; Loos, P.-F. Excitation energies from diffusion Monte Carlo using selected configuration interaction nodes. *J. Chem. Phys.* **2018**, *149*, 034108.

(110) Loos, P. F.; Scemama, A.; Blondel, A.; Garniron, Y.; Caffarel, M.; Jacquemin, D. A Mountaineering Strategy to Excited States:

Highly-Accurate Reference Energies and Benchmarks. *J. Chem. Theory Comput.* **2018**, *14*, 4360.

(111) Garniron, Y.; Scemama, A.; Giner, E.; Caffarel, M.; Loos, P. F. Selected Configuration Interaction Dressed by Perturbation. *J. Chem. Phys.* **2018**, *149*, 064103.

(112) Evangelista, F. A. Adaptive multiconfigurational wave functions. *J. Chem. Phys.* **2014**, *140*, 124114.

(113) Schriber, J. B.; Evangelista, F. A. Communication: An adaptive configuration interaction approach for strongly correlated electrons with tunable accuracy. *J. Chem. Phys.* **2016**, *144*, 161106.

(114) Tubman, N. M.; Lee, J.; Takeshita, T. Y.; Head-Gordon, M.; Whaley, K. B. A deterministic alternative to the full configuration interaction quantum Monte Carlo method. *J. Chem. Phys.* **2016**, *145*, 044112.

(115) Liu, W.; Hoffmann, M. R. iCI: Iterative CI toward full CI. *J. Chem. Theory Comput.* **2016**, *12*, 1169–1178.

(116) Per, M. C.; Cleland, D. M. Energy-based truncation of multi-determinant wavefunctions in quantum Monte Carlo. *J. Chem. Phys.* **2017**, *146*, 164101.

(117) Ohtsuka, Y.; Hasegawa, J.-y. Selected configuration interaction method using sampled first-order corrections to wave functions. *J. Chem. Phys.* **2017**, *147*, 034102.

(118) Zimmerman, P. M. Incremental full configuration interaction. *J. Chem. Phys.* **2017**, *146*, 104102.

(119) Blunt, N. S. An efficient and accurate perturbative correction to initiator full configuration interaction quantum Monte Carlo. *J. Chem. Phys.* **2018**, *148*, 221101.

(120) Budzák, S.; Scalmani, G.; Jacquemin, D. Accurate Excited-State Geometries: a CASPT2 and Coupled-Cluster Reference Database for Small Molecules. *J. Chem. Theory Comput.* **2017**, *13*, 6237–6252.

(121) Aidas, K.; et al. The Dalton Quantum Chemistry Program System. *WIREs Comput. Mol. Sci.* **2014**, *4*, 269–284.

(122) Stanton, J. F.; Gauss, J.; Cheng, L.; Harding, M. E.; Matthews, D. A.; Szalay, P. G.; with contributions from Auer, A. A.; Bartlett, R. J.; Benedikt, U.; Berger, C.; Bernholdt, D. E.; Bomble, Y. J.; Christiansen, O.; Engel, F.; Faber, R.; Heckert, M.; Heun, O.; Hilgenberg, M.; Huber, C.; Jagau, T.-C.; Jonsson, D.; Jusélius, J.; Kirsch, T.; Klein, K.; Lauderdale, W. J.; Lipparini, F.; Metzroth, T.; Mück, L. A.; O'Neill, D. P.; Price, D. R.; Prochnow, E.; Puzzarini, C.; Ruud, K.; Schiffmann, F.; Schwalbach, W.; Simmons, C.; Stopkowitz, S.; Tajti, A.; Vázquez, J.; Wang, F.; Watts, J. D.; and the integral packages MOLECULE (Almlöf, J.; Taylor, P. R.), PROPS (Taylor, P. R.), ABACUS (Helgaker, T.; Jensen, H. J. Aa.; Jørgensen, P.; Olsen, J.), and ECP routines Mitin, A. V.; van Wüllen, C. *CFOUR, Coupled-Cluster techniques for Computational Chemistry*, quantum-chemical program package. For the current version, see <http://www.cfour.de>.

(123) Francs, M. M.; Pietro, W. J.; Hehre, W. J.; Binkley, J. S.; Gordon, M. S.; DeFrees, D. J.; Pople, J. A. Self-Consistent Molecular Orbital Methods. XXIII. A polarization-type basis set for second-row elements. *J. Chem. Phys.* **1982**, *77*, 3654.

(124) Dunning, T. H., Jr. Gaussian basis sets for use in correlated molecular calculations. I. The atoms boron through neon and hydrogen. *J. Chem. Phys.* **1989**, *90*, 1007.

(125) Kállay, M.; Gauss, J. Calculation of Excited-State Properties Using General Coupled-Cluster and Configuration-Interaction Models. *J. Chem. Phys.* **2004**, *121*, 9257–9269.

(126) Kállay, M.; Rolik, Z.; Csontos, J.; Nagy, P.; Samu, G.; Mester, D.; Csóka, J.; Szabó, B.; Ladjánszki, I.; Szegedy, L.; Ladóczki, B.; Petrov, K.; Farkas, M.; Mezei, P. D.; Hégyel, B. *MRCC, Quantum Chemical Program*; 2017; see www.mrcc.hu.

(127) Werner, H.-J.; Knowles, P. J.; Knizia, G.; Manby, F. R.; Schütz, M. Molpro: a general-purpose quantum chemistry program package. *Wiley Interdisciplinary Reviews: Computational Molecular Science* **2012**, *2*, 242–253.

(128) Finley, J.; Malmqvist, P.-A.; Roos, B. O.; Serrano-Andrés, L. The Multi-State CASPT2 Method. *Chem. Phys. Lett.* **1998**, *288*, 299–306.

(129) Shiozaki, T.; Györfy, W.; Celani, P.; Werner, H.-J. Communication: Extended Multi-State Complete Active Space

Second-Order Perturbation Theory: Energy and Nuclear Gradients. *J. Chem. Phys.* **2011**, *135*, 081106.

(130) Caffarel, M.; Applencourt, T.; Giner, E.; Scemama, A. Using CIPSI Nodes in Diffusion Monte Carlo. *Recent Progress in Quantum Monte Carlo*; American Chemical Society: Washington, DC, USA, 2016; Chapter 2, pp 15–46, DOI: [10.1021/bk-2016-1234.ch002](https://doi.org/10.1021/bk-2016-1234.ch002).

(131) Scemama, A.; Applencourt, T.; Garniron, Y.; Giner, E.; David, G.; Caffarel, M. *Quantum Package*, v1.0; 2016; https://github.com/LCPQ/quantum_package.

(132) Saha, B.; Ehara, M.; Nakatsuji, H. Singly and Doubly Excited States of Butadiene, Acrolein, and Glyoxal: Geometries and Electronic Spectra. *J. Chem. Phys.* **2006**, *125*, 014316.

(133) Christiansen, O.; Koch, H.; Halkier, A.; Jørgensen, P.; Helgaker, T.; Sánchez de Merás, A. Large-scale Calculations of Excitation Energies in Coupled Cluster Theory: The Singlet Excited States of Benzene. *J. Chem. Phys.* **1996**, *105*, 6921–6939.

(134) Gálvez, F. J.; Buendía, E.; Sarsa, A. Excited States of Beryllium Atom from Explicitly Correlated Wave Functions. *J. Chem. Phys.* **2002**, *117*, 6071–6082.

(135) Dallos, M.; Lischka, H. A Systematic Theoretical Investigation of the Lowest Valence- and Rydberg-Excited Singlet States of Trans-Butadiene. The Character of the $1^1B_u(V)$ State Revisited. *Theor. Chem. Acc.* **2004**, *112*, 16–26.

(136) Boschen, J. S.; Theis, D.; Ruedenberg, K.; Windus, T. L. Accurate ab Initio Potential Energy Curves and Spectroscopic Properties of the Four Lowest Singlet States of C_2 . *Theor. Chem. Acc.* **2014**, *133*, 1425.

(137) Barbatti, M.; Paier, J.; Lischka, H. Photochemistry of Ethylene: A Multireference Configuration Interaction Investigation of The Excited-State Energy Surfaces. *J. Chem. Phys.* **2004**, *121*, 11614.

(138) Angeli, C.; Cimraglia, R.; Cestari, M. A Multireference N-Electron Valence State Perturbation Theory Study Of The Electronic Spectrum Of S-Tetrazine. *Theor. Chem. Acc.* **2009**, *123*, 287–298.

(139) Silva-Junior, M. R.; Schreiber, M.; Sauer, S. P. A.; Thiel, W. Benchmarks of Electronically Excited States: Basis Set Effects Benchmarks of Electronically Excited States: Basis Set Effects on CASPT2 Results. *J. Chem. Phys.* **2010**, *133*, 174318.

(140) Schreiber, M.; Silva-Junior, M. R.; Sauer, S. P. A.; Thiel, W. Benchmarks for Electronically Excited States: CASPT2, CC2, CCSD and CC3. *J. Chem. Phys.* **2008**, *128*, 134110.

(141) Mulliken, R. S. Note on Electronic States of Diatomic Carbon, and the Carbon-Carbon Bond. *Phys. Rev.* **1939**, *56*, 778–781.

(142) Clementi, E.; McLean, A. D. SCF-LCAO-MO Wave Function for the $1^1\Sigma_g +$ Ground State of C_3 . *J. Chem. Phys.* **1962**, *36*, 45–47.

(143) Abrams, M. L.; Sherrill, C. D. Full Configuration Interaction Potential Energy Curves for the $X^1\Sigma_g^+$, $B^1\Delta_g$, and $B'^1\Sigma_g^+$ States of C_2 : A Challenge for Approximate Methods. *J. Chem. Phys.* **2004**, *121*, 9211–9219.

(144) Sherrill, C. D.; Piecuch, P. The $X^1\Sigma_g^+$, $B^1\Delta_g$, and $B'^1\Sigma_g^+$ States of C_2 : A Comparison of Renormalized Coupled-Cluster and Multireference Methods with Full Configuration Interaction Benchmarks. *J. Chem. Phys.* **2005**, *122*, 124104.

(145) Angeli, C.; Cimraglia, R.; Pastore, M. A Comparison of Various Approaches in Internally Contracted Multireference Configuration Interaction: The Carbon Dimer as a Test Case. *Mol. Phys.* **2012**, *110*, 2963–2968.

(146) Blunt, N. S.; Smart, S. D.; Booth, G. H.; Alavi, A. An Excited-State Approach within Full Configuration Interaction Quantum Monte Carlo. *J. Chem. Phys.* **2015**, *143*, 134117.

(147) Boggio-Pasqua, M.; Voronin, A.; Halvick, P.; Rayez, J.-C. Analytical Representations of High Level Ab Initio Potential Energy Curves of the C_2 Molecule. *J. Mol. Struct.: THEOCHEM* **2000**, *531*, 159–167.

(148) Sharma, S. A General Non-Abelian Density Matrix Renormalization Group Algorithm with Application to the C_2 Dimer. *J. Chem. Phys.* **2015**, *142*, 024107.

(149) Booth, G. H.; Cleland, D.; Thom, A. J. W.; Alavi, A. Breaking the Carbon Dimer: The Challenges of Multiple Bond Dissociation with

Full Configuration Interaction Quantum Monte Carlo Methods. *J. Chem. Phys.* **2011**, *135*, 084104.

(150) Mahapatra, U. S.; Chattopadhyay, S.; Chaudhuri, R. K. Molecular Applications of State-Specific Multireference Perturbation Theory to HF, H₂O, H₂S, C₂, and N₂ Molecules. *J. Chem. Phys.* **2008**, *129*, 024108.

(151) Purwanto, W.; Zhang, S.; Krakauer, H. Excited State Calculations Using Phaseless Auxiliary-Field Quantum Monte Carlo: Potential Energy Curves of Low-Lying C₂ Singlet States. *J. Chem. Phys.* **2009**, *130*, 094107.

(152) Shi, D.; Zhang, X.; Sun, J.; Zhu, Z. MRCI Study on Spectroscopic and Molecular Properties of B¹Δ_g, C¹g⁺, and I¹Δ_g Electronic States of the C₂ Radical. *Mol. Phys.* **2011**, *109*, 1453–1465.

(153) Su, P.; Wu, J.; Gu, J.; Wu, W.; Shaik, S.; Hiberty, P. C. Bonding Conundrums in the C₂ Molecule: A Valence Bond Study. *J. Chem. Theory Comput.* **2011**, *7*, 121–130.

(154) Toulouse, J.; Umrigar, C. J. Full Optimization of Jastrow–Slater Wave Functions with Application to the First-Row Atoms and Homonuclear Diatomic Molecules. *J. Chem. Phys.* **2008**, *128*, 174101.

(155) Varandas, A. J. C. Extrapolation to the Complete-Basis-Set Limit and the Implications of Avoided Crossings: The X¹Σ⁺g⁺, B¹Δ_{1g}, and B¹Σ⁺g⁺ States of C₂. *J. Chem. Phys.* **2008**, *129*, 234103.

(156) Sokolov, A. Y.; Chan, G. K.-L. A Time-Dependent Formulation of Multi-Reference Perturbation Theory. *J. Chem. Phys.* **2016**, *144*, 064102.

(157) Wouters, S.; Poelmans, W.; Ayers, P. W.; Van Neck, D. CheMPS2: A Free Open-Source Spin-Adapted Implementation of the Density Matrix Renormalization Group for Ab Initio Quantum Chemistry. *Comput. Phys. Commun.* **2014**, *185*, 1501–1514.

(158) Ahmed, K.; Balint-Kurti, G. G.; Western, C. M. Ab Initio Calculations and Vibrational Energy Level Fits for the Lower Singlet Potential-Energy Surfaces of C₃. *J. Chem. Phys.* **2004**, *121*, 10041–10051.

(159) Carter, S.; Mills, I.; Murrell, J. Analytical Functions for the Ground State Potential Surfaces of And. *J. Mol. Spectrosc.* **1980**, *81*, 110–121.

(160) Carter, S.; Mills, I.; Dixon, R. Potential Energy Surface Intersections for Triatomic Molecules. *J. Mol. Spectrosc.* **1984**, *106*, 411–422.

(161) Chabalowski, C. F.; Buenker, R. J.; Peyerimhoff, S. D. Ab initio Study of the Locations and Intensities of the Lowest-lying Electronic Transitions of the C₃ and C₂ O Molecules. *J. Chem. Phys.* **1986**, *84*, 268–274.

(162) Clementi, E.; Clementi, H. Electron Distributions in Small Molecules. *J. Chem. Phys.* **1962**, *36*, 2824–2833.

(163) Hoffmann, R. Extended Hückel Theory—V. *Tetrahedron* **1966**, *22*, 521–538.

(164) Jensen, P. The Potential Energy Surface for the C₃ Molecule Determined from Experimental Data. Evidence for a Bent Equilibrium Structure. *Collect. Czech. Chem. Commun.* **1989**, *54*, 1209–1218.

(165) Jensen, P.; Rohlfing, C. M.; Almlöf, J. Calculation of the Complete-active-space Self-consistent-field Potential-energy Surface, the Dipole Moment Surfaces, the Rotation–Vibration Energies, and the Vibrational Transition Moments for C₃ (X¹Σ⁺g⁺). *J. Chem. Phys.* **1992**, *97*, 3399–3411.

(166) Jorgensen, U. G.; Almlöf, J.; Siegbahn, P. E. M. Complete Active Space Self-Consistent Field Calculations of the Vibrational Band Strengths for C₃. *Astrophys. J.* **1989**, *343*, 554.

(167) Kraemer, W.; Bunker, P.; Yoshimine, M. A Theoretical Study of the Rotation–Vibration Energy Levels and Dipole Moment Functions of CCN⁺, CNC⁺, and C₃. *J. Mol. Spectrosc.* **1984**, *107*, 191–207.

(168) Liskow, D. H.; Bender, C. F.; Schaefer, H. F. Bending Frequency of the C₃ Molecule. *J. Chem. Phys.* **1972**, *56*, 5075–5080.

(169) Mebel, A. M.; Kaiser, R. I. An Ab Initio Study on the Formation of Interstellar Tricarbon Isomers. *Chem. Phys. Lett.* **2002**, *360*, 139.

(170) Mladenović, M.; Schmatz, S.; Botschwina, P. Large-scale Ab Initio Calculations for C₃. *J. Chem. Phys.* **1994**, *101*, 5891–5899.

(171) Monninger, G.; Förderer, M.; Gürtler, P.; Kalhofer, S.; Petersen, S.; Nemes, L.; Szalay, P. G.; Krätschmer, W. Vacuum Ultraviolet Spectroscopy of the Carbon Molecule C₃ in Matrix Isolated State: Experiment and Theory. *J. Phys. Chem. A* **2002**, *106*, 5779–5788.

(172) Murrell, J. N. The Many-Body Expansion of the Potential Energy Function for Elemental Clusters. *Int. J. Quantum Chem.* **1990**, *37*, 95–102.

(173) Perić-Radić, J.; Römelt, J.; Peyerimhoff, S.; Buenker, R. Configuration Interaction Calculation of the Potential Curves for the C₃ Molecule in Its Ground and Lowest-Lying Πu States. *Chem. Phys. Lett.* **1977**, *50*, 344–350.

(174) Pitzer, K. S.; Clementi, E. Large Molecules in Carbon Vapor. *J. Am. Chem. Soc.* **1959**, *81*, 4477.

(175) Rocha, C. M. R.; Varandas, A. J. C. Accurate Ab Initio -Based Double Many-Body Expansion Potential Energy Surface for the Adiabatic Ground-State of the C₃ Radical Including Combined Jahn-Teller plus Pseudo-Jahn-Teller Interactions. *J. Chem. Phys.* **2015**, *143*, 074302.

(176) Rocha, C. M. R.; Varandas, A. J. C. The Jahn-Teller plus Pseudo-Jahn-Teller Vibronic Problem in the C₃ Radical and Its Topological Implications. *J. Chem. Phys.* **2016**, *144*, 064309.

(177) Römelt, J.; Peyerimhoff, S. D.; Buenker, R. J. Ab Initio MRD CI Calculations for the Electron Spectrum of the C₃ Radical. *Chem. Phys. Lett.* **1978**, *58*, 1–7.

(178) Saha, S.; Western, C. M. Experimental and Ab Initio Study of a New D~Δg¹ State of the C₃ Radical. *J. Chem. Phys.* **2006**, *125*, 224307.

(179) Schröder, B.; Sebald, P. High-Level Theoretical Rovibrational Spectroscopy beyond Fc-CCSD(T): The C₃ Molecule. *J. Chem. Phys.* **2016**, *144*, 044307.

(180) Spirko, V.; Mengel, M.; Jensen, P. Calculation of Rotation–Vibration Energy Levels in Ground State C₃ by a Born–Oppenheimer-Type Separation of the Vibrational Motions. *J. Mol. Spectrosc.* **1997**, *183*, 129–138.

(181) Terentyev, A.; Scholz, R.; Schreiber, M.; Seifert, G. Theoretical Investigation of Excited States of C₃. *J. Chem. Phys.* **2004**, *121*, 5767–5776.

(182) Varandas, A. J. C. Extrapolation to the Complete-Basis-Set Limit and the Implications of Avoided Crossings: The X¹Σ⁺g⁺, B¹Δ_{1g}, and B¹Σ⁺g⁺ States of C₂. *J. Chem. Phys.* **2008**, *129*, 234103.

(183) Varandas, A. A Simple, yet Reliable, Direct Diabatization Scheme. The 1Σ⁺g⁺ States of C₂. *Chem. Phys. Lett.* **2009**, *471*, 315–321.

(184) Varandas, A. J. C.; Rocha, C. M. R. C_n (n = 2–4): Current Status. *Philos. Trans. R. Soc., A* **2018**, *376*, 20170145.

(185) Yousaf, K. E.; Taylor, P. R. On the Electronic Structure of Small Cyclic Carbon Clusters. *Chem. Phys.* **2008**, *349*, 58–68.

(186) Fukuto, J. M.; Switzer, C. H.; Miranda, K. M.; Wink, D. A. NITROXYL (HNO): Chemistry, Biochemistry, and Pharmacology. *Annu. Rev. Pharmacol. Toxicol.* **2005**, *45*, 335–355.

(187) Miranda, K. M. The Chemistry of Nitroxyl (HNO) and Implications in Biology. *Coord. Chem. Rev.* **2005**, *249*, 433–455.

(188) Williams, G. A. Theoretical Study of the Excited States of the Nitroxyl Radical (HNO) via the Equations of Motion Method. *Chem. Phys. Lett.* **1975**, *30*, 495–497.

(189) Luna, A.; Merchán, M.; Ross, B. O. A Theoretical Analysis of the Lowest Excited States in HNO/NOH and HPO/POH. *Chem. Phys.* **1995**, *196*, 437–445.

(190) Ehara, M.; Oyagi, F.; Abe, Y.; Fukuda, R.; Nakatsuji, H. Excited-State Geometries and Vibrational Frequencies Studied Using the Analytical Energy Gradients of the Direct Symmetry-Adapted Cluster–Configuration Interaction Method. I. HAX-Type Molecules. *J. Chem. Phys.* **2011**, *135*, 044316.

(191) Lacombe, S.; Loudet, M.; Dargelos, A.; Camou, J. Calculation of the Electronic and Photoelectronic Spectra of Nitroso Compounds: A Reinvestigation by Use of Configuration Interaction Methods. *Chem. Phys.* **2000**, *258*, 1–12.

(192) Dolgov, E. K.; Bataev, V. A.; Pupyshev, V. I.; Godunov, I. A. Ab Initio Description of the Structure and Dynamics of the Nitrosomethane Molecule in the First Excited Singlet and Triplet Electronic States. *Int. J. Quantum Chem.* **2004**, *96*, 589–597.

- (193) Dolgov, E. K.; Bataev, V. A.; Godunov, I. A. Structure of the Nitrosomethane Molecule (CH_3NO) in the Ground Electronic State: Testing of Ab Initio Methods for the Description of Potential Energy Surface. *Int. J. Quantum Chem.* **2004**, *96*, 193–201.
- (194) Arenas, J. F.; Otero, J. C.; Peláez, D.; Soto, J. CASPT2 Study of the Decomposition of Nitrosomethane and Its Tautomerization Reactions in the Ground and Low-Lying Excited States. *J. Org. Chem.* **2006**, *71*, 983–991.
- (195) Robin, M. B. In *Higher Excited States of Polyatomic Molecules*; Robin, M. B., Ed.; Academic Press, 1985; Vol. III.
- (196) Watts, J. D.; Gwaltney, S. R.; Bartlett, R. J. Coupled-cluster Calculations of the Excitation Energies of Ethylene, Butadiene, and Cyclopentadiene. *J. Chem. Phys.* **1996**, *105*, 6979–6988.
- (197) Angeli, C. On the Nature of the $\pi \rightarrow \pi^*$ Ionic Excited States: The V State of Ethene as a Prototype. *J. Comput. Chem.* **2009**, *30*, 1319–1333.
- (198) Feller, D.; Peterson, K. A.; Davidson, E. R. A Systematic Approach to Vertically Excited States of Ethylene Using Configuration Interaction and Coupled Cluster Techniques. *J. Chem. Phys.* **2014**, *141*, 104302.
- (199) Head-Gordon, M.; Rico, R. J.; Oumi, M.; Lee, T. J. A Doubles Correction To Electronic Excited States From Configuration Interaction In The Space Of Single Substitutions. *Chem. Phys. Lett.* **1994**, *219*, 21.
- (200) Shen, J.; Li, S. Block Correlated Coupled Cluster Method with the Complete Active-Space Self-Consistent-Field Reference Function: Applications for Low-Lying Electronic Excited States. *J. Chem. Phys.* **2009**, *131*, 174101.
- (201) Caricato, M.; Trucks, G. W.; Frisch, M. J.; Wiberg, K. B. Electronic Transition Energies: A Study of the Performance of a Large Range of Single Reference Density Functional and Wave Function Methods on Valence and Rydberg States Compared to Experiment. *J. Chem. Theory Comput.* **2010**, *6*, 370–383.
- (202) Leang, S. S.; Zahariev, F.; Gordon, M. S. Benchmarking the Performance of Time-Dependent Density Functional Methods. *J. Chem. Phys.* **2012**, *136*, 104101.
- (203) Hoyer, C. E.; Ghosh, S.; Truhlar, D. G.; Gagliardi, L. Multiconfiguration Pair-Density Functional Theory Is as Accurate as CASPT2 for Electronic Excitation. *J. Phys. Chem. Lett.* **2016**, *7*, 586–591.
- (204) Giner, E.; Angeli, C. Metal-Ligand Delocalization and Spin Density in the CuCl_2 and $[\text{CuCl}_4]^{2-}$ Molecules: Some Insights from Wave Function Theory. *J. Chem. Phys.* **2015**, *143*, 124305.
- (205) Merchán, M.; Roos, B. O. A Theoretical Determination of the Electronic Spectrum of Formaldehyde. *Theor. Chem. Acc.* **1995**, *92*, 227–239.
- (206) Paterson, M. J.; Christiansen, O.; Pawłowski, F.; Jørgensen, P.; Hättig, C.; Helgaker, T.; Salek, P. Benchmarking Two-Photon Absorption with CC3 Quadratic Response Theory, and Comparison with Density-Functional Response Theory. *J. Chem. Phys.* **2006**, *124*, 054322.
- (207) Müller, T.; Lischka, H. Simultaneous Calculation of Rydberg and Valence Excited States of Formaldehyde. *Theor. Chem. Acc.* **2001**, *106*, 369–378.
- (208) Foresman, J. B.; Head-Gordon, M.; Pople, J. A.; Frisch, M. J. Toward a Systematic Molecular Orbital Theory for Excited States. *J. Phys. Chem.* **1992**, *96*, 135–149.
- (209) Hadad, C. M.; Foresman, J. B.; Wiberg, K. B. Excited States of Carbonyl Compounds. 1. Formaldehyde and Acetaldehyde. *J. Phys. Chem.* **1993**, *97*, 4293–4312.
- (210) Head-Gordon, M.; Maurice, D.; Oumi, M. A Perturbative Correction to Restricted Open-Shell Configuration-Interaction with Single Substitutions for Excited-States of Radicals. *Chem. Phys. Lett.* **1995**, *246*, 114–121.
- (211) Gwaltney, S. R.; Bartlett, R. J. An Application of the Equation-Of-Motion Coupled Cluster Method to the Excited States of Formaldehyde, Acetaldehyde, and Acetone. *Chem. Phys. Lett.* **1995**, *241*, 26–32.
- (212) Wiberg, K. B.; Stratmann, R. E.; Frisch, M. J. A Time-Dependent Density Functional Theory Study of the Electronically Excited States of Formaldehyde, Acetaldehyde and Acetone. *Chem. Phys. Lett.* **1998**, *297*, 60–64.
- (213) Wiberg, K. B.; de Oliveira, A. E.; Trucks, G. A Comparison of the Electronic Transition Energies for Ethene, Isobutene, Formaldehyde, and Acetone Calculated Using RPA, TDDFT, and EOM-CCSD. Effect of Basis Sets. *J. Phys. Chem. A* **2002**, *106*, 4192–4199.
- (214) Peach, M. J. G.; Benfield, P.; Helgaker, T.; Tozer, D. J. Excitation Energies in Density Functional Theory: an Evaluation and a Diagnostic Test. *J. Chem. Phys.* **2008**, *128*, 044118.
- (215) Li, X.; Paldus, J. Multi-Reference State-Universal Coupled-Cluster Approaches to Electronically Excited States. *J. Chem. Phys.* **2011**, *134*, 214118.
- (216) Daday, C.; Smart, S.; Booth, G. H.; Alavi, A.; Filippi, C. Full Configuration Interaction Excitations of Ethene and Butadiene: Resolution of an Ancient Question. *J. Chem. Theory Comput.* **2012**, *8*, 4441–4451.
- (217) Hsu, C.-P.; Hirata, S.; Head-Gordon, M. Excitation Energies from Time-Dependent Density Functional Theory for Linear Polyene Oligomers: Butadiene to Decapentaene. *J. Phys. Chem. A* **2001**, *105*, 451–458.
- (218) Kitao, O.; Nakatsuji, H. Cluster Expansion of the Wavefunction: Valence and Rydberg Excitations of Trans- and Cis-Butadiene. *Chem. Phys. Lett.* **1988**, *143*, 528–534.
- (219) McDiarmid, R.; Sheybani, A.-H. Reinterpretation of the Main Absorption Band of 1,3-butadiene. *J. Chem. Phys.* **1988**, *89*, 1255–1261.
- (220) Mosher, O. A.; Flicker, W. M.; Kuppermann, A. Electronic Spectroscopy of *S-trans* 1,3-butadiene by Electron Impact. *J. Chem. Phys.* **1973**, *59*, 6502–6511.
- (221) Ostojić, B.; Domcke, W. Ab Initio Investigation of the Potential Energy Surfaces Involved in the Photochemistry of *S-Trans*-1,3-Butadiene. *Chem. Phys.* **2001**, *269*, 1–10.
- (222) Strodel, P.; Tavan, P. A Revised MRCI-Algorithm Coupled to an Effective Valence-Shell Hamiltonian. II. Application to the Valence Excitations of Butadiene. *J. Chem. Phys.* **2002**, *117*, 4677–4683.
- (223) Dash, M.; Moroni, S.; Scemama, A.; Filippi, C. Perturbatively selected configuration-interaction wave functions for efficient geometry optimization in quantum Monte Carlo. *J. Chem. Theory Comput.* **2018**, *14*, 4176.
- (224) Send, R.; Valsson, O.; Filippi, C. Electronic Excitations of Simple Cyanine Dyes: Reconciling Density Functional and Wave Function Methods. *J. Chem. Theory Comput.* **2011**, *7*, 444–455.
- (225) Boulanger, P.; Jacquemin, D.; Duchemin, I.; Blase, X. Fast and Accurate Electronic Excitations in Cyanines with the Many-Body Bethe-Salpeter Approach. *J. Chem. Theory Comput.* **2014**, *10*, 1212–1218.
- (226) Le Guennic, B.; Jacquemin, D. Taking Up the Cyanine Challenge with Quantum Tools. *Acc. Chem. Res.* **2015**, *48*, 530–537.
- (227) Dykstra, C. E.; Lucchese, R. R.; Schaefer, H. F. Electron Correlation Effects on the Excitation Energies of the Lowest Triplet States of Glyoxal. *J. Chem. Phys.* **1977**, *67*, 2422.
- (228) Ha, T.-K. Ab Initio Calculation of Cis-Trans Isomerization in Glyoxal. *J. Mol. Struct.* **1972**, *12*, 171–178.
- (229) Hirao, K. Direct Cluster Expansion Method. Application to Glyoxal. *J. Chem. Phys.* **1983**, *79*, 5000–5010.
- (230) Hollauer, E.; Nascimento, M. A. C. A CASSCF Description of the $N\pi^*$ Singlet and Triplet Electronic Excited States of the Trans-Glyoxal Molecule. *Chem. Phys. Lett.* **1991**, *181*, 463–466.
- (231) Pincell, U.; Cadioli, B.; David, D. A Theoretical Study of the Electronic Structure and Conformation of Glyoxal. *J. Mol. Struct.* **1971**, *9*, 173–176.
- (232) Aquilante, F.; Barone, V.; Roos, B. O. A Theoretical Investigation of Valence and Rydberg Electronic States of Acrolein. *J. Chem. Phys.* **2003**, *119*, 12323–12334.
- (233) Bouabça, T.; Ben Amor, N.; Maynaud, D.; Caffarel, M. A Study of the Fixed-Node Error in Quantum Monte Carlo Calculations of Electronic Transitions: The Case of the Singlet $N \rightarrow \pi^*$ (CO) Transition of the Acrolein. *J. Chem. Phys.* **2009**, *130*, 114107.

- (234) Guareschi, R.; Filippi, C. Ground- and Excited-State Geometry Optimization of Small Organic Molecules with Quantum Monte Carlo. *J. Chem. Theory Comput.* **2013**, *9*, 5513–5525.
- (235) Buenker, R. J.; Peyerimhoff, S. D. CI Method for the Study of General Molecular Potentials. *Theor. Chem. Acc.* **1968**, *12*, 183–199.
- (236) Peyerimhoff, S. D.; Buenker, R. J. Comparison of the Molecular Structure and Spectra of Benzene and Borazine. *Theor. Chim. Acta* **1970**, *19*, 1–19.
- (237) Hay, P. J.; Shavitt, I. *Ab Initio* Configuration Interaction Studies of the π -Electron States of Benzene. *J. Chem. Phys.* **1974**, *60*, 2865–2877.
- (238) Palmer, M. H.; Walker, I. C. The Electronic States of Benzene and the Azines. I. The Parent Compound Benzene. Correlation of Vacuum UV and Electron Scattering Data with *Ab Initio* CI Studies. *Chem. Phys.* **1989**, *133*, 113–121.
- (239) Kitao, O.; Nakatsuji, H. Cluster Expansion of the Wave Function. Valence and Rydberg Excitations and Ionizations of Benzene. *J. Chem. Phys.* **1987**, *87*, 1169–1182.
- (240) Lorentzon, J.; Malmqvist, P.-A.; Fiilscher, M.; Roos, B. O. A CASPT2 Study of the Valence and Lowest Rydberg Electronic States of Benzene and Phenol. *Theor. Chim. Acta* **1995**, *91*, 91–108.
- (241) Hashimoto, T.; Nakano, H.; Hirao, K. Theoretical Study of the Valence $\Pi \rightarrow \pi^*$ Excited States of Polyacenes: Benzene and Naphthalene. *J. Chem. Phys.* **1996**, *104*, 6244–6258.
- (242) Christiansen, O.; Stanton, J. F.; Gauss, J. A Coupled Cluster Study of the 1 1A_{1g} and 1 1B_{2u} States of Benzene. *J. Chem. Phys.* **1998**, *108*, 3987–4001.
- (243) Handy, N. C.; Tozer, D. J. Excitation Energies of Benzene from Kohn-Sham Theory. *J. Comput. Chem.* **1999**, *20*, 106–113.
- (244) Hald, K.; Jørgensen, P.; Christiansen, O.; Koch, H. Implementation of Electronic Ground States and Singlet and Triplet Excitation Energies in Coupled Cluster Theory with Approximate Triples Corrections. *J. Chem. Phys.* **2002**, *116*, 5963–5970.
- (245) Palmer, M. H.; Walker, I. C. The Electronic States of the Azines. V. Pyridazine, Studied by VUV Absorption, near Threshold Electron Energy-Loss Spectroscopy and *Ab Initio* Multi-Reference Configuration Interaction Calculations. *Chem. Phys.* **1991**, *157*, 187–200.
- (246) Fulscher, M. P.; Andersson, K.; Roos, B. O. Toward an Accurate Molecular Orbital Theory for Excited States: The Azabenzenes. *J. Phys. Chem.* **1992**, *96*, 9204–9212.
- (247) Durig, J.; Whang, C.; Attia, G.; Li, Y. Microwave Spectra, Structure, and Barrier to Internal Rotation of CH₃SnH₂D, CH₃SnHD₂ and CH₃SnD₃. *J. Mol. Spectrosc.* **1984**, *108*, 240–248.
- (248) Fulscher, M. P.; Roos, B. O. The Excited States of Pyrazine: A Basis Set Study. *Theor. Chem. Acc.* **1994**, *87*, 403–413.
- (249) Weber, P.; Reimers, J. R. *Ab Initio* and Density Functional Calculations of the Energies of the Singlet and Triplet Valence Excited States of Pyrazine. *J. Phys. Chem. A* **1999**, *103*, 9821–9829.
- (250) Nooijen, M. Similarity Transformed Equation of Motion Coupled-Cluster Study of Excited States of Selected Azabenzenes. *Spectrochim. Acta, Part A* **1999**, *55*, 539–559.
- (251) Mason, S. F. 248. The Electronic Spectra of N-Heteroaromatic Systems. Part IV. The Vibrational Structure of the N \rightarrow π Band of Sym-Tetrazine. *J. Chem. Soc.* **1959**, *0*, 1263–1268.
- (252) Innes, K.; Ross, I.; Moomaw, W. R. Electronic States of Azabenzenes and Azanaphthalenes: A Revised and Extended Critical Review. *J. Mol. Spectrosc.* **1988**, *132*, 492–544.
- (253) Fridh, C.; Åsbrink, L.; Jonsson, B.; Lindholm, E. Rydberg Series in Small Molecules. *Int. J. Mass Spectrom. Ion Phys.* **1972**, *9*, 485–497.
- (254) Palmer, M. H.; McNab, H.; Reed, D.; Pollacchi, A.; Walker, I. C.; Guest, M. F.; Siggel, M. R. The Molecular and Electronic States of 1,2,4,5-Tetrazine Studied by VUV Absorption, near-Threshold Electron Energy-Loss Spectroscopy and *Ab Initio* Multi-Reference Configuration Interaction Studies. *Chem. Phys.* **1997**, *214*, 191–211.
- (255) Livak, D.; Innes, K. A Triplet-Singlet Transition of s-Tetrazine. *J. Mol. Spectrosc.* **1971**, *39*, 115–122.
- (256) Rubio, M.; Roos, B. O. A Theoretical Study of the Electronic Spectrum of S-Tetrazine. *Mol. Phys.* **1999**, *96*, 603–615.
- (257) Nooijen, M. Electronic Excitation Spectrum of s-Tetrazine: An Extended-STEOM-CCSD Study. *J. Phys. Chem. A* **2000**, *104*, 4553–4561.
- (258) Harbach, P. H. P.; Wormit, M.; Dreuw, A. The Third-Order Algebraic Diagrammatic Construction Method (ADC(3)) for the Polarization Propagator for Closed-Shell Molecules: Efficient Implementation and Benchmarking. *J. Chem. Phys.* **2014**, *141*, 064113.
- (259) Flicker, W. M.; Mosher, O. A.; Kuppermann, A. Low Energy, Variable Angle Electron-Impact Excitation of 1,3,5-Hexatriene. *Chem. Phys. Lett.* **1977**, *45*, 492–497.
- (260) Nakayama, K.; Nakano, H.; Hirao, K. Theoretical Study of the $\pi \rightarrow \pi^*$ Excited States of Linear Polyenes: The Energy Gap between 1¹B_u⁺ and 2¹A_g[?] States and Their Character. *Int. J. Quantum Chem.* **1998**, *66*, 157–175.